Accepted Manuscript published as ERC-23-0312.R1. Accepted for publication: 11-Apr-2024

GPNMB Promotes Tumor Growth and is a Biomarker for Lymphangioleiomyomatosis

Erin Gibbons[1,2], Manisha Taya[3], Huixing Wu[4], Samia H Lopa[5], Joel Moss[6], Elizabeth P Henske[7], Francis X McCormack[4], Stephen R Hammes[1,2,*]

[1]Department of Microbiology and Immunology University of Rochester School of Medicine and Dentistry, Rochester, NY 14642, USA, [2]Division of Endocrinology, Diabetes, and Metabolism, Department of Medicine, University of Rochester School of Medicine and Dentistry, Rochester, NY 14642, USA, [3]Division of Hematology and Oncology, UT Southwestern, Dallas, TX 75390, USA, [4]Division of Pulmonary, Critical Care and Sleep Medicine, University of Cincinnati, Cincinnati, Ohio 45267, USA, [5]Department of Biostatistics and Computational Biology, University of Rochester, [6]Pulmonary Branch, National Heart, Lung, and Blood Institute (NHLBI), NIH, Bethesda, Maryland 20892, USA, [7]Pulmonary and Critical Care Medicine, Brigham and Women's Hospital, Harvard Medical School, Boston, MA 02115, USA

*Corresponding Author: 601 Elmwood, Ave., Rochester, NY 14642, Email: Stephen_hammes@urmc.rochester.edu

Short Title: GPNMB is a biomarker and enhancer of LAM

Key Words: Biomarker, GPNMB, Lymphangioleiomyomatosis, mTORC1

Word Count: 5408 words

Abstract

Lymphangioleiomyomatosis (LAM) is a rare, progressive cystic lung disease affecting almost exclusively female-sexed individuals. The cysts represent regions of lung destruction caused by smooth muscle tumors containing mutations in one of the two tuberous sclerosis (*TSC*) genes. mTORC1 inhibition slows but does not stop LAM advancement. Furthermore, monitoring disease progression is hindered by insufficient biomarkers. Therefore, new treatment options and biomarkers are needed. LAM cells express melanocytic markers, including Glycoprotein Non-Metastatic Melanoma Protein B (GPNMB). The function of GPNMB in LAM is currently unknown; however, GPNMB's unique cell surface expression on tumor versus benign cells makes GPNMB a potential therapeutic target, and persistent release of its extracellular ectodomain suggests potential as a serum biomarker. Here we establish that GPNMB expression is dependent on mTORC1 signaling, and that GPNMB regulates TSC2-null tumor cell invasion *in-vitro*. Further, we demonstrate that GPNMB enhances TSC2-null xenograft tumor growth *in-vivo*, and that ectodomain release is required for this xenograft growth. We also show that GPNMB's ectodomain is released from the cell surface of TSC2-null cells by proteases ADAM10 and 17, and we identify the protease target sequence on GPNMB. Finally, we demonstrate that GPNMB's ectodomain is present at higher levels in LAM patient serum compared to healthy controls, and that ectodomain levels decrease with mTORC1 inhibition, making it a potential LAM biomarker.

Accepted Manuscript published as ERC-23-0312.R1. Accepted for publication: 11-Apr-2024

Introduction

Lymphangioleiomyomatosis (LAM) is a rare cystic lung disease impacting almost exclusively female-sexed persons. Cyst walls are comprised of a myriad of small smooth muscle cell tumors that cause LAM lung pathology (McCormack et al., 2012; Prizant & Hammes, 2016). Tumor growth and cyst development lead to progressive pulmonary function loss, especially during reproductive years and during pregnancy, sometimes requiring lung transplantation (Karbowniczek et al., 2003; Taveira-DaSilva et al., 2020). LAM tumors contain mutations in one of the tuberous sclerosis complex genes (*TSC1* or *TSC2*), either from inherited Tuberous Sclerosis Complex (TSC) disease, or from sporadic mutations, leading to constitutive mTORC1 activation and subsequent cell hyperproliferation (Astrinidis et al., 2000; Carsillo et al., 2000; McCormack et al., 2012; Strizheva et al., 2001). Importantly, tumors recur after lung transplantation, and LAM cells are found in circulating body fluids (Karbowniczek et al., 2003), suggesting a metastatic nature of LAM, and begging the question as to the origin of lung LAM cells.

Diagnosing sporadic LAM (in individuals without TSC) is difficult, as symptoms and CT findings share commonalities with other pulmonary disorders, making lung biopsy sometimes necessary (Ryu et al., 2006). Currently, Vascular Endothelial Growth Factor-D (VEGF-D) is the only serum biomarker for LAM, with about two-thirds of biopsy proven LAM patients having diagnostic levels of VEGF-D. However, VEGF-D levels are not always consistent with LAM tumor burden or disease severity, presenting a need for new LAM biomarkers (Nijmeh et al., 2018).

One way of identifying LAM in tissue samples is to measure expression of melanocytic markers. Melanocytic markers, expressed primarily in melanocytes, are upregulated in some cancers such as melanoma, triple negative breast cancer (TNBC), and LAM. One specific melanocytic marker used to diagnose LAM is pre-melanosome 17 (PMEL17) (Kuhnen et al., 2001). Another melanocytic marker is Glycoprotein Non-Metastatic Protein B (GPNMB), which was first discovered to be relevant to LAM from mRNA sequencing of uterine tumors from a

uterine-specific TSC2-null mouse model (Prizant et al., 2016). GPNMB is highly expressed in TSC2-null cell lines, as well as in tumors from lungs and uteri of LAM patients (Prizant et al., 2016). GPNMB is reported to promote migration, invasion, and proliferation in various cancers (Rose, Annis, et al., 2010; Weterman et al., 1995; Zhang et al., 2017), and high expression is sometimes associated with poorer prognosis (Hoashi et al., 2010; Huang et al., 2021). Notably, scRNAseq from LAM patient lungs demonstrated that GPNMB is one of the most differentially expressed genes in LAM^{CORE} cells (Guo et al., 2020).

While GPNMB is intracellular in primary somatic cells, it is expressed intracellularly and on the cell membrane of melanoma, breast cancer, glioblastoma and LAM tumor cells, making it a potential cell surface drug target (Kuan et al., 2006; Prizant et al., 2016). In fact, CDX-011, a GPNMB specific antibody-drug conjugate, has been used in melanoma clinical trials (Maric et al., 2013; Vaklavas & Forero, 2014). Interestingly, the extracellular GPNMB ectodomain is cleaved and shed, with evidence suggesting that the ectodomain may promote metastasis in prostate, lung, pancreatic and breast cancers (Maric et al., 2013; Oyewumi et al., 2016; Rose et al., 2017; Torres et al., 2015). Based on these observations, we hypothesized that GPNMB may promote LAM tumor progression, and that the GPNMB ectodomain is a potential LAM biomarker.

Here we demonstrate that GPNMB enhances TSC2-null xenograft tumor growth in mice, perhaps by increasing tumor cell invasive potential. We find that *GPNMB* mRNA and GPNMB protein expression increase under serum starvation and that GPNMB expression is dependent on mTORC1 activity. We describe ADAM (A-Disintegrin-And-Metalloproteinase) 10 and 17 as enzymes that release the GPNMB ectodomain, identify the ADAM10/17 target site on the GPNMB protein, and demonstrate that ectodomain cleavage is important for TSC2-null tumor growth and invasion. Finally, we show that the GPNMB ectodomain is detectable in LAM patient serum and decreases with sirolimus treatment, indicating that GPNMB may serve as a new biomarker for LAM diagnosis and treatment efficacy.

Accepted Manuscript published as ERC-23-0312.R1. Accepted for publication: 11-Apr-2024

Materials and Methods

Cell culture and treatments

Human *TSC2*-null 621-101 cells derived from a LAM patient renal angiomyolipoma were from Elizabeth Henske, Brigham and Women's Hospital. Rat *Tsc2*-null ELT3 cells derived from a rat leiomyoma were from Cheryl Walker, Texas A&M Health Science Center. Rat ELT3-Luc cells expressing luciferase were from Jane Yu, University of Cincinnati. Mouse LTM3 cells were cloned from uterine-specific TSC2-null mouse uteri (Minor et al., 2023). Cells were cultured in DF8 media with base of DMEM+F12 media (1:1) (11320033 Gibco, Billings MO) and additives (Howe et al., 1995). Cells were maintained at 37°C, 5% CO2 and passaged every 4-5 days. Cells were treated with 5μM Actinomycin D (ActD) (A1410, Sigma, St. Louis, Missouri) (vehicle-DMSO), 20nM Rapamycin (R-5000 LC-Laboratories, Woburn, Massachusetts) (vehicle-ethanol), GI254023X (GIX) (SML0789, Millipore-Sigma) (vehicle DMSO), or TAPI-1 (B4686 ApexBio, Houston, TX) (vehicle-DMSO).

CRISPR-mediated GPNMB knockout and control clone generation

CRISPR/Cas9-mediated GPNMB knockout and non-targeting control cell lines were generated in ELT3-Luc cells by JetPrime® transfection (101000015 Polylus, Illkirch, France) and sgRNA CRISPR/Cas9 All-in-One Non-Viral Vector set plasmids (abmgood, Vancouver, Canada) with GPNMB (K7535627) or non-targeting control guide-sgRNA (K094) and GFP tagged Cas9 nuclease. GFP-positive cells were selected, seeded in 96-well plates, and clones evaluated for GPNMB protein and mRNA. Human GPNMB and non-cleavable GPNMB expression in GPNMB-null rat ELT3 cells were generated by transfection and selecting GPNMB-positive clones.

Mouse Studies

Mouse studies were performed following AALAC guidelines and approved by the University of Rochester Committee on Animal Resources. For xenografts, 6–8-week-old female SCID-NOD mice (001803, Jackson Laboratory, Bar Harbor, ME) were subcutaneously injected with 2×10^6 ELT3-Luc or 1.94×10^6 621-101 cells in 0.1 mL of a 1:1 mixture of Matrigel (356234, Corning, Corning, NY) and PBS. For Sup Fig 5, 1ug/kg CDX-011 (Celldex Therapeutics, Needham, MA) or PBS was subcutaneously injected into NOD-SCID mice once a week for 5-weeks. Treatment began at 12-weeks post injection (when tumors were palpable) and ended at 17-weeks, with mice sacrificed at 19-weeks.

Western Blots

Cell lysates were collected in 2x-sample buffer containing 2-mercaptoethanol. Media was concentrated using 30k centrifugal devices (MCP030C41, Microsep® Advance Centrifugal Devices Pall Corporation, Port Washington, NY) (UFC803024, Amicon® Ultra-4 Centrifugal Filter Unit, Millipore Sigma) and mixed with NuPAGE™ LDS 4x-Sample Buffer containing 2-mercaptoethanol. Tissue samples were lysed in RIPA buffer (#89900, Thermo-Fisher-Scientific, Waltham, MA) supplemented with 1×Halt™ protease and phosphatase-inhibitor cocktail (78430, Thermo-Fisher-Scientific) and mixed with 2x-sample buffer. Samples were boiled for 5-minutes, loaded onto 4%-15% gradient polyacrylamide gels (4561084, Bio-Rad, Hercules, CA), and then transferred to PVDF membranes (#1620177, Bio-Rad). Blots were blocked using 5% milk in TBST. Primary antibodies were: 1:500 GPNMB (AF2550-SP R&D Biosystems, Minneapolis, MN), 1:4000 GAPDH (14C10, Cell Signaling), 1:1000 pS6 (S235/236, Cell Signaling), 1:1000 tS6 (5G10, Cell Signaling, Danvers, MA). Secondary antibodies were: 1:2000 Rabbit anti-goat (#1721034, Biorad) and 1:4000 Goat anti-rabbit (#1706515, Biorad). ECL Prime Western Blotting Detection Reagent (RPN2236, Cytiva, Marlborough, MA) or Clarity Western ECL Substrate (1705062, Bio-Rad) were used, and intensities determined using ImageJ.

Accepted Manuscript published as ERC-23-0312.R1. Accepted for publication: 11-Apr-2024

Immunohistochemistry

Mouse tissue was paraffin-embedded and sectioned into 5-micron sections. Samples were deparaffinized and rehydrated in a graded alcohol series. For antibody staining, 1:200 Ki67 (D3B5, Cell Signaling) and 1:200 Goat-anti rabbit secondary antibody (BA-1000, Vector Laboratories, Newark, CA) were used. Images were acquired using an Olympus IX71 inverted microscope and cellSens software. For connective tissue staining, Trichrome Collagen Stain Kit (ab150686, Abcam, Cambridge, United Kingdom) was utilized. Images were taken using Aperio Imagescope and analyzed with the trichrome extension.

Immunofluorescence

Mouse tumor tissue was prepared as above. 1:100 dilution of goat-anti-human GPNMB (AF2550-SP, R&D Biosystems) and 1:200 Alexa-Fluor-488-conuugated anti-goat IgG (705-545-147, Jackson ImmunoResearch) were used. Nuclei were labeled with 1μg/mL Hoechst (33258, Invitrogen, Waltham, MA). Images were acquired as above.

Celigo Image Cytometer Proliferation Assay

2000 ELT3 or ELT3-Luc cells were plated into a 24-well Falcon Polystyrene Microplate (Corning) in 500μL DF8 media and images taken using the Celigo image cytometer (Nexcelom Bioscience, Lawrence, MA) at 24, 48, and 72-hours, and quantified using Celigo software. For ELT3 cell studies with collagen coating, 9.87 μg/cm^2 collagen solution from bovine skin (C4243, Sigma) was used.

Real-time Quantitative Polymerase Chain Reaction (RT-qPCR)

Total RNA was extracted using the RNeasy Plus Mini Kit (74134, QIAGEN, Hilden, Germany). RT-qPCR reactions used qScript RT-qPCR Tough Mix (89236-672, Quantabio, Beverly, MA) and TaqMan primers (Applied Biosystems, Waltham, MA). The StepOne plus Real-

Time PCR system (Applied Biosystems) was used. mRNA levels were normalized to GAPDH and analyzed using the ΔΔCt method. TaqMan primers were: mouse *Gpnmb* (Mm01328587_m1) human *Gpnmb* (Hs01095669_m1), rat *Gpnmb* (Rn00591060_m1), mouse *Gapdh* (Mm99999915_g1), human *Gapdh* (Hs02786624_g1), and rat *Gapdh* (Rn01775763_g1).

Small interfering RNA (siRNA) transfection

ON-TARGETplus siRNA SMARTPOOLs (Dharmacon, Lafayette, CO) for human GPNMB (L-011741-01-0005), mouse GPNMB (L-040019-01-0005), rat GPNMB (L-091754-02-0005), human ADAM10 (L-004503-00-0005), human ADAM17 (L-003453-00-0005), or nonspecific pool (NSP) (D-001810-10) were transfected into cells using Lipofectamine™ RNAiMAX (#13778075, Thermo Fisher Scientific).

Thymidine Incorporation Assay (BRDU)

1,5-bromo-2′-deoxyuridine (BrdU) Cell Proliferation Assay kit (6813S, Cell Signaling Technology) was used. Conditions were optimized for each cell line. 1000 and 2000 cells/well were plated in a 96-well plate and grown 48-hours in DF8 media containing 10% FBS. siRNA specific for GPNMB or nonspecific siRNA (Dharmacon) was added to the cells after 24-hours and BRDU reagent added for 24-hours. Absorbance was read at 450nm.

3-(4,5-dimethylthiazol-2-yl)-2,5-diphenyl tetrazolium bromide (MTT) Assay

2000-cells were plated into 96-well plates and treated with siRNA the following day. 72-hours after transfection, MTT was added and 4-hours later solubilization solution added (11465007001, Sigma). Cells were grown in DF8 media containing 10% FBS. Signals were measured at 550nm and 690nm.

Accepted Manuscript published as ERC-23-0312.R1. Accepted for publication: 11-Apr-2024

Transwell Migration and Invasion Assays

50,000 ELT3, and 100,000 LTM3,621-101 or ELT3-Luc mutant GPNMB cells were plated in serum-free DF8 media in the top chamber and DF8 media containing 10% FBS added to the bottom chamber. Cells were allowed to migrate for 16-18 hours and invade for 24-hours. Migration assays were performed using 6.5mm-diameter, 8-μm pore-size transwell inserts (Corning). Invasion assays were the same, but with Matrigel-coated transwells. Cells were fixed in 4% paraformaldehyde for 10-minutes and stained with 1% crystal violet (V5625, Sigma). Transwells were rinsed in water and cells scraped off the top of wells with cotton swabs. Each condition was performed in duplicate. To quantify, 5-images at 10x objective were taken with the Olympus IX71 inverted microscope and cellSens software and averaged for each transwell. For ELT3 cell migration, images were quantified using Photoshop CS3 extended measurement. For ELT3 cell invasion, ImageJ analyze particles function was used. For 621-101 and LTM3 cells, the number of migrated or invaded cells were quantified using ImageJ.

Site-Directed Mutagenesis

Human *GPNMB* RNA was isolated from 621-101 cells, reverse-transcribed into DNA, and cloned into the pcDNA3.1+ plasmid. The Q5 mutagenesis kit (E0554S, New England BioLabs) was utilized to delete the VRR sequence. JetPrime transfection was used to express wild-type or mutant-GPNMB in ELT3-Luc GPNMB-knockout cells.

Flow Cytometry

ELT3-Luc cells were harvested using Cell Stripper and stained with 10μg/mL GPNMB antibody for 1-hour, then Alexa-Fluor 488 ant-goat secondary antibody for 30-minutes, then fixed prior to running on the flow cytometer.

Human Samples

De-identified human serum samples were obtained from patients seen at Brigham and Young Hospital (Elizabeth Henske and Joel Moss, National Institutes of Health) and from patients who enrolled in the MILES trial (Frank McCormack) (McCormack et al., 2011).

Enzyme-linked immunosorbent assay (ELISA)

Human or mouse serum samples or concentrated cell media samples were used. GPNMB was measured using a GPNMB ELISA kit (DY2550, R&D Systems) and DuoSet ELISA Ancillary Reagent Kit 2 (DY008B, R&D Systems). Absorbance was read at 450nm with a reference wavelength of 570nm.

Statistical Analysis

Data are represented +/-SEM. p-values are indicated: *$p<0.05$; **$p<0.01$, ***$p<0.001$, ****$p<0.0001$; $p>0.05$ was considered not significant (ns). GPNMB levels for control and LAM patients were not normally distributed with some outliers. To compare between these two groups, we used a non-parametric two-sample Wilcoxon (Mann-Whitney) test. For the paired analysis of 10 patients, we used a non-parametric paired signed rank test to test if GPNMB values significantly decreased three-months after Sirolimus treatment. For sensitivity, we applied the paired t-test on the log-transformed (base-10) GPNMB values. MILES data were analyzed using generalized linear mixed models with a random intercept to account for the correlation between time. To detect a differential drop-out pattern between sirolimus and placebo groups, a mixed effect logistic regression model was fit with data missing or not (binary) as the dependent variable, and random intercept, treatment (sirolimus vs. placebo), time (categorical), and their interaction, as independent variables. We tested if the proportion with data across various timepoints was significantly different between two treatment groups (treatment and time interaction test) from this model. Then we fit a linear mixed model with log-transformed GPNMB values as the dependent

Accepted Manuscript published as ERC-23-0312.R1. Accepted for publication: 11-Apr-2024

variable, and a random intercept, treatment (sirolimus vs. placebo), time (categorical), and their interaction as independent variables. An interaction test assessed whether the change over time was significantly different between sirolimus and placebo groups. Pairwise changes between time-points were assessed using least-square mean differences from this model.

Results

GPNMB knockdown suppresses TSC2-null cell invasion without affecting other *in-vitro* processes.

In melanoma, TNBC, and other cancers, GPNMB promotes tumor progression (Hoashi et al., 2010; Huang et al., 2021). To examine GPNMB's role mediating tumor cell functions, we determined effects of GPNMB knockdown on proliferation, migration, and invasion *in-vitro*. Non-specific (NSP) or GPNMB-targeted siRNAs were transfected into TSC2-null rat ELT3 cells and assays performed looking at processes associated with tumor growth and metastasis (Fig 1). We employed transient siRNA-mediated knockdown to reduce potential compensatory mechanisms in cultured knockout cells. Knockdown was confirmed by western blot (Fig 1A). GPNMB knockdown had no effect on proliferation by BRDU incorporation or cell counting on a collagen-coated plate (Fig 1B, C). In contrast, by MTT, we observed a small but statistically significant decrease in metabolic rate with GPNMB-knockdown compared to NSP (Fig 1D). Migration was unaffected by GPNMB-knockdown (Fig 1E, F). However, invasion through Matrigel-coated membranes showed a modest but significant decrease with GPNMB knockdown (Fig 1G, H). Similar GPNMB knockdown studies using TSC2-null mouse LTM3 (Minor et al., 2023) and TSC2-null human 621-101 cells demonstrated no differences in proliferation, metabolic rate, or migration (Sup Fig 1, 2). Like ELT3 cells, LTM3 cells demonstrated significant reduction in invasion with GPNMB-knockdown (Sup Fig 1G). Invasion by 621-101 cells trended downward with GPNMB-knockdown, but was not statistically significant, perhaps because of 621-101's low invasive potential (Sup Fig 2G). To determine why GPNMB-knockdown reduced invasion, we examined epithelial-to-mesenchymal transition markers in ELT3 cells but saw no differences (not shown). Interestingly, *Mmp9* mRNA levels in ELT3 cells and *Mmp2* mRNA levels in LTM3 cells were reduced with GPNMB-knockdown, suggesting that GPNMB might enhance invasion via upregulation of MMP2/9 expression (Sup Fig 3).

Accepted Manuscript published as ERC-23-0312.R1. Accepted for publication: 11-Apr-2024

GPNMB enhances TSC2-null xenograft tumor growth.

Given reduced invasion in ELT3 cells with GPNMB knockdown, we moved to an *in-vivo* model to examine GPNMB effects on ELT3 xenograft growth. We used CRISPR/Cas9 to knockout GPNMB expression in TSC2-null ELT3-Luc cells by transfecting with either sgRNA specific for GPNMB or a non-targeting sgRNA control. Clones with GPNMB mRNA Ct values above 37 (low to no expression), as well as undetectable GPNMB by western blot, were expanded. GPNMB knockout clones were verified to have similar growth relative to control cells *in-vitro* prior to injecting into mice (Sup Fig 4A). Cells were injected into both leg flanks of SCID-NOD mice and tumor volume monitored. To compensate for clonal differences, two different clonal GPNMB knockout cell lines as well as the polyclonal knockout cell line (before diluting to individual clones) were utilized. These were combined in the analysis as knockout (KO). Similarly, two non-targeting control clonal cell lines, the non-targeting polyclonal cell line, and parent ELT3-Luc cells were combined as controls. GPNMB knockout was verified in final xenograft tissue by western blot and immunofluorescence (Fig 2A, B). Representative images are in Figure 2A, but all tumors were verified for presence or absence of GPNMB by western. Average tumor volume and final tumor weight were significantly decreased in GPNMB knockout xenografts (Fig 2C, D). Like *in-vitro* cell growth assays, *in-vivo* proliferation was unchanged in the absence of GPNMB, as demonstrated by Ki67 staining of three representative control and GPNMB knockout xenografts (Sup Fig 4B, C). Changes in apoptosis and vascularization were also no different. In contrast, we observed significantly more collagen in GPNMB knockout xenografts relative to controls, suggesting GPNMB may modulate fibroblast actions in the tumor microenvironment (Fig 2E, F).

Since genetic knockdown of GPNMB significantly reduced TSC2-null xenograft growth, we next determined whether drug targeting of GPNMB similarly reduced xenograft growth. We utilized the experimental anti-human GPNMB immunoglobulin-drug conjugate, CDX-011, which has been used in clinical trials for treatment of GPNMB-expressing breast cancer and melanoma (Pollack et al., 2007; Qian et al., 2008; Tse et al., 2006; Vaklavas & Forero, 2014). Since CDX-

011 is directed against human GPNMB, we injected human TSC2-null human 621-101 cells in SCID-NOD mice. Once tumors were palpable in all mice, mice were treated with vehicle or CDX-011 and tumor volumes monitored weekly. No tumors grew in drug-treated mice, while all tumors grew in control mice (Sup Fig 5A, B). Importantly, GPNMB ectodomain was detected by ELISA in serum of all control, but no CDX-011 treated mice (Sup Fig 5C). Although the sample size was small due to limited drug availability, these data confirm the importance of GPNMB for tumor growth and demonstrate that GPNMB is a potential cell surface target for TSC2-null tumors.

Serum starvation increases GPNMB in a transcription- and mTORC1-dependent manner.

Previous work demonstrated that GPNMB was expressed in TSC2-null cells and TSC2-null uteri and decreased in mice treated with rapamycin (Prizant et al., 2016). Here we further dissected GPNMB expression in TSC2-null cells. *In-vitro*, when TSC2-null cells are grown without serum, GPNMB increased both at mRNA and protein levels (Fig 3A, D). *Gpnmb* mRNA expression increased over 3-fold in serum-starved ELT3 cells compared to cells grown in complete media, and remained elevated when serum was added back for 10-minutes, 30-minutes, 1-hour, or 24-hours (Fig 3A). Protein expression as shown by a representative western blot, was similar, except that by 24-hours GPNMB protein was decreased (Fig 3D). Enhancement of GPNMB protein and mRNA expression with serum starvation was due to transcription, as Actinomycin D (ActD) abrogated enhancing effects of serum starvation (Fig 3B, E). Importantly, *Gpnmb* mRNA and GPNMB protein expression in ELT3 cells growing under any condition was dependent on mTORC1 signaling, as treatment with rapamycin almost completely abrogated GPNMB expression in complete media and serum starvation conditions (Fig 3C, F, G). Phosphorylated S6 was diminished with rapamycin, verifying the drug was working (Fig 3F). Similar results were observed in TSC2-null mouse LTM3 and human 621-101 cells (Sup Fig 6). Notably, experiments were performed to determine specific mechanisms of serum starvation dependent increases in GPNMB, including analyzing PI3K and MAPK pathways; however,

 Accepted Manuscript published as ERC-23-0312.R1. Accepted for publication: 11-Apr-2024

inhibition of these pathways did not alter the increase in GPNMB expression (data not shown). Importantly, mTORC1 signaling remained robust with serum starvation, as no significant changes in pS6 were detected (Fig 3F, H, Sup Fig 6C, E, H, J).

The GPNMB ectodomain is cleaved by Adam10 and 17 proteases.

The GPNMB ectodomain is released from the cell surface of cancer cells (Hoashi et al., 2010). Accordingly, we detected GPNMB ectodomain in the serum of mice with human 621-101 xenografts (Sup Fig 5C). In breast cancer, ADAM10 has been implicated as at least partially responsible for ectodomain cleavage (Rose, Annis, et al., 2010). Therefore, we sought to definitively determine whether ADAM10 and/or related ADAM17 protease promoted GPNMB ectodomain release in TSC2-null cells. We focused on human GPNMB, given its relevance to human disease and because human GPNMB ectodomain is more readily detectable by ELISA and western blot. ADAM10 and 17 were knocked down in 621-101 cells using siRNA. Knockdown efficiency was measured by reduced mRNA expression; approximately 85% for ADAM10 and 68% for ADAM17 (Fig 4A, B). GPNMB in cell lysates and media was detected by western blot, and amount of shed GPNMB relative to lysate GPNMB calculated. GPNMB shedding was significantly reduced when either ADAM10 or ADAM17 expression was knocked down, indicating that both enzymes were important for ectodomain shedding (Fig 4C, D). We verified siRNA results through pharmacological inhibition of ADAM10 with GIX and ADAM17 with TAPI. Both inhibitors reduced ectodomain shedding like siRNA knockdown (Fig 4E-G). The combination of ADAM10 and 17 inhibitions did not further decrease GPNMB shedding, perhaps due to incomplete enzymatic inhibition (Fig 4G). Together, these knockdown and pharmacologic studies demonstrate that ADAM10 and ADAM17 are important mediators of GPNMB ectodomain release.

Identification of the GPNMB ectodomain cleavage site and demonstration of its importance in tumor growth and invasion.

Having identified the primary enzymes cleaving GPNMB, we next turned toward their target. Protein sequencing of GPNMB ectodomain suggested that cleavage occurred at or near a conserved VRR sequence (Fig 5A, (Furochi et al., 2007)). We therefore created a VRR deletion mutation in human GPNMB and transfected GPNMB-null ELT3-Luc cells with mock DNA, cDNA expressing wild-type (WT) GPNMB, or cDNA expressing the VRR deletion mutant. Western blot of media and lysate GPNMB demonstrated absence of GPNMB in knockout cells, two bands in wild-type GPNMB-transfected cells (likely a mature and less mature form), and one band in the VRR deletion mutant (likely the less mature form) (Fig 5C)(Hoashi et al., 2010). Notably, cell surface staining verified that the VRR deletion mutant was expressed on the cell surface similarly to WT GPNMB (Fig 5B). However, while present at the cell surface, VRR-deleted GPNMB was unable to shed its ectodomain, as shown by Western blot (Fig 5C) and ELISA (Fig 5D), confirming that the VRR sequence is critical for GPNMB ectodomain cleavage. We did a similar xenograft experiment to Figure 2 with two wildtype-GPNMB and two mutant GPNMB-expressing clones in ELT3 cells lacking endogenous GPNMB. Average tumor volume over time and final tumor weight were significantly greater in the wildtype- compared to mutant-GPNMB expressing cells (Fig 6A, B). We detected GPNMB ectodomain by ELISA in the serum of mice with wildtype but not mutant-GPNMB-expressing tumors (Fig 6C). Next, we used one clone expressing mutant-GPNMB and knocked down GPNMB expression by siRNA (Fig 6D-E). Unlike Figure 1, where ELT3 cells expressing native GPNMB showed decreased invasion with GPNMB-knockdown, knockdown of mutant-GPNMB had no effect on invasion (Fig 6F-G), suggesting that GPNMB-cleavage is required to enhance ELT3 cell invasion. Together, these results demonstrate that GPNMB-cleavage is critical for TSC2-null cell *in-vivo* growth and invasion.

Serum GPNMB ectodomain is a LAM biomarker and novel marker of sirolimus treatment response.

Accepted Manuscript published as ERC-23-0312.R1. Accepted for publication: 11-Apr-2024

We have shown that GPNMB is highly expressed in LAM patient lung and uterine tissue, and we can detect shed GPNMB in blood of mice (Sup Fig 5C, Fig 6C (Prizant et al., 2016)). Therefore, we examined GPNMB ectodomain levels in serum of multiple LAM patient populations. In our initial cohort of 30 healthy controls and 30 LAM patients, serum GPNMB levels were significantly elevated in LAM patients versus controls (Fig 7A), though there was overlap between groups. We next examined a cohort of 10 LAM patients with specimens obtained prior to initiation of sirolimus treatment and 3-months after onset of treatment (Fig 7B). Here we saw a significant decrease in serum GPNMB post treatment. This decrease was present in 8/10 patients and, for the two patients in whom GPNMB did not decrease, GPNMB levels were low to start. Finally, we examined serum samples from the Multicenter International LAM Efficacy with Sirolimus (MILES) trial (McCormack et al., 2011). Prior to treatment (0-months), the placebo and sirolimus groups had similar levels of GPNMB (Fig 7E). However, at 6-months and 12-months post treatment, sirolimus-treated patients had significantly less GPNMB, indicating a beneficial response to treatment. Of note, treatment was stopped at 12-months and patients monitored for another year. At 24-months the difference between groups was no longer significant (Fig 7E). This was also demonstrated when graphing each patient separately (Fig 7C, D). These data demonstrate that GPNMB levels are higher when patients are not taking sirolimus, and that serum GPNMB ectodomain levels can be used to monitor response to treatment.

Discussion

Melanocytic markers are upregulated in LAM tissues and have been used as histological markers (Kuhnen et al., 2001). However, while melanocytic markers like PMEL-17 are useful for differentiating LAM from other cystic lung diseases in tissue samples, they have not proven useful as serum biomarkers to diagnose and follow LAM progression and treatment. In fact, the only serum biomarker used in LAM is VEGF-D, which is helpful but has limitations regarding sensitivity and correlation with disease severity (Li et al., 2022; Young et al., 2013). Our laboratory became interested in the melanocytic maker GPNMB because it promotes tumor growth and metastasis in some cancers, often portending worse prognosis (Kuan et al., 2006; Maric et al., 2013; Rose, Grosset, et al., 2010; Taya & Hammes, 2018). Furthermore, when expressed on the cell surface, GPNMB's extracellular ectodomain is constitutively released, making it a potential serum biomarker (Maric et al., 2013). We first discovered GPNMB expression in a uterine-specific TSC2-null mouse model for LAM, and then confirmed GPNMB expression both intracellularly and on the plasma membranes of TSC2-null cell lines (Prizant et al., 2016). We then demonstrated GPNMB expression in human LAM lung and uterine tumors (Prizant et al., 2016). More recently, scRNA sequencing of LAM lungs confirmed that GPNMB is one of the most highly differentially expressed genes in LAM cells (Guo et al., 2020). Together, these data suggested that GPNMB may serve as both a biomarker and a regulator LAM tumor growth. Indeed, here we demonstrated that GPNMB promotes TSC2-null tumor growth, and that expression of its ectodomain in blood serves as a LAM biomarker.

Initial *in-vitro* studies using TSC2-null cell lines from three different species demonstrated no effects of GPNMB knockdown on proliferation and migration. However, GPNMB knockdown significantly reduced invasion in rat TSC2-null ELT3 and mouse TSC2-null LTM3 cells, with similar magnitude, but not statistically significant, reduction in human TSC2-null 621-101 cells (Fig 1, Sup 1, 2). These differences were enough to prompt examination of GPNMB knockout in ELT3 xenografts, where we saw significant reduction of tumor growth with GPNMB knockout (Fig

Accepted Manuscript published as ERC-23-0312.R1. Accepted for publication: 11-Apr-2024

2). Furthermore, treatment of mice with the GPNMB-specific antibody drug conjugate, CDX-011, abrogated growth of TSC2-null human 621-101 cells (Sup Fig 5). While interpretation of the latter study is limited due to restrictions in drug supply, together, these data indicate that GPNMB supports TSC2-null xenograft growth, and that it is a potential treatment target. Based on the *in-vitro* invasion studies as well as the increased collagen in the smaller GPNMB-null ELT3 xenografts, we postulate that GPNMB may play a role in tumor cell invasion, consistent with other cancer models where GPNMB increases invasion and metastasis (Fiorentini et al., 2014; Maric et al., 2015; Oyewumi et al., 2016; Rich et al., 2003; Rose et al., 2007). GPNMB binds integrins and facilitates adherence to the extracellular matrix, which could further drive tumor progression and metastasis (Maric et al., 2015; Oyewumi et al., 2016). Additionally, GPNMB may be anti-fibrotic in scleroderma fibrosis (Palisoc et al., 2022), which could explain why GPNMB inhibited collagen formation in GPNMB-expressing relative to GPNMB-null xenografts. However, GPNMB's role may more be more nuanced depending on context, as GPNMB has also been shown to promote pulmonary fibrosis (Wang et al., 2023). We demonstrated that *Mmp* mRNA decreases when GPNMB is knocked down, consistent with data in other cancers where GPNMB increased MMPs, invasion, and metastasis ((Fiorentini et al., 2014; Rich et al., 2003).

Another potential alternative mechanism whereby GPNMB may promote TSC2-null tumor growth *in-vivo* but not *in-vitro* involves inhibition of T cell-mediated tumor cell death. Cell surface and soluble GPNMB from monocytes and macrophages has been shown to interact with Syndecan-4 on T cells to inhibit their cytotoxic activity, which would in turn permit increased tumor growth (Chung et al., 2014; Liguori et al., 2021; Ripoll et al., 2007; Tomihari et al., 2010). Accordingly, blocking GPNMB actions on immunosuppressive monocytes from cancer patients may permit T cells to regain their anti-tumor functions (Kobayashi, 2018). Therefore, it is possible that, as with PD-L1 expression in tumor cells, cell surface expression of GPNMB on TSC2-null cells, or perhaps even GPNMB ectodomain, might suppress cytotoxic T cell actions, to allow tumor progression.

Although GPNMB's role in promoting TSC2-null cell invasion and tumor progression is important, one of the most interesting and potentially useful aspects of GPNMB expression in tumor cells is its expression on the cell membrane and constitutive shedding of its ectodomain (Furochi et al., 2007; Hoashi et al., 2010; Rose, Annis, et al., 2010). Therefore, we sought to determine how the GPNMB ectodomain is released in TSC2-null cells. ADAM10 has been reported to release soluble GPNMB in breast cancer cells (Rose, Annis, et al., 2010). Here we found that both ADAM10 and ADAM17 were responsible for GPNMB shedding through siRNA-mediated knockdown and drug inhibition of the proteases (Fig 4). While both strategies implicate ADAM10 and 17 in ectodomain cleavage, we were unable to completely abrogate ectodomain release, most likely due to incomplete knockdown and/or enzyme inhibition, though it remains possible that other proteases can release the GPNMB-ectodomain. Regarding the ADAM10/17 targets on GPNMB, previous work suggested that the cleavage sequence of GPNMB occurs at or near a VRR sequence (Furochi et al., 2007). Since this region is well conserved, we utilized site-directed mutagenesis to delete the VRR sequence in human GPNMB. In doing so, we definitively demonstrated that, while GPNMB was still expressed on the cell surface, its ectodomain was no longer shed into the media of TSC2-null cells (Fig 5). Thus, our studies have revealed both the primary proteases and their target sites on GPNMB. TSC2-null cells expressing non-cleavable GPNMB have minimal tumor growth *in-vivo*, suggesting either that GPNMB ectodomain release is necessary to promote tumor growth *in-vivo* or that uncleavable GPNMB inhibits TSC2-null tumor growth *in-vivo* (Fig 6). Further studies will examine these possibilities; however, these results suggest that inhibiting ectodomain release of GPNMB using ADAM10/17 inhibitors or blocking antibodies that have been utilized in other cancers could be therapeutic strategies in LAM (Saha et al., 2019).

Constitutive release of the GPNMB ectodomain suggests that its detection in the serum of patients with LAM or other GPNMB-expressing cancers might serve as a biomarker. While GPNMB expression in cells has been utilized as a histological marker, and possibly prognostic

Accepted Manuscript published as ERC-23-0312.R1. Accepted for publication: 11-Apr-2024

predictor for tumors such as TNBC (Huang et al., 2021), to our knowledge, GPNMB ectodomain has not been documented as a serum biomarker in any cancer. In contrast, and as proof of principle that measuring ectodomain levels in human serum can be done, detection of serum GPNMB ectodomain has been demonstrated in humans with non-cancerous diseases such as diabetes mellitus, Gaucher disease, and nonalcoholic steatohepatitis (Huo et al., 2023; Katayama et al., 2015; Murugesan et al., 2018). GPNMB is also elevated in the cerebral spinal fluid of Alzheimer's and Adrenoleukodystrophy (ALD) patients (Aichholzer et al., 2021; Taghizadeh et al., 2022). Here we find that GPNMB ectodomain levels are higher in LAM patients versus controls, with some overlap between the two groups, demonstrating for the first time that the GPNMB ectodomain may serve as a biomarker for GPNMB-expressing cancers (Fig 7). As mentioned, VEGF-D is the only serum biomarker used for LAM (McCormack et al., 2016; Nijmeh et al., 2018; Young et al., 2013). Analysis of the MILES trial, which was the first randomized controlled study that showed sirolimus as an effective treatment for LAM, found that VEGF-D decreased with sirolimus treatment, but remained unchanged in placebo treated patients (Young et al., 2013). In the same population, we similarly found that serum GPNMB ectodomain levels significantly decreased during sirolimus treatment, but not in placebo treatment (Fig 7). In addition, during the final 12 months of the trial when sirolimus was stopped, GPNMB levels began to rise. These results are consistent with our findings that GPNMB expression is dependent on mTORC1, and demonstrate that, like VEGF-D, GPNMB may be useful in tracking effects of sirolimus in LAM patients. Notably, in patients with pneumothorax, a common complication of LAM, VEGF-D levels started at a lower baseline, making it a less applicable biomarker in this population (Young et al., 2013). Other limitations of VEGF-D are that it has low sensitivity and studies have shown varying ranges of cut off levels and diagnostic performances (Glasgow et al., 2009; Li et al., 2022; McCormack et al., 2016). Future studies will be necessary to determine whether serum GPNMB ectodomain levels, in combination with other markers such as VEGF-D, will become standard approaches for diagnosing and monitoring LAM patients on and off treatment.

Declaration of Interest

There are no conflicts of interest that could be perceived as prejudicing the impartiality of the research reported.

Funding

EG was supported by NIH T32HL066988. SRH was supported by DOD grant TS220024 and NIH R01CA193583. JM was supported by Intramural Research, NIH, NHLBI. EPH, HW, and FXM were supported by NIH U01HL131022.

Acknowledgements

We would like to acknowledge Tara Vrooman, Christina Seger, and Zhiguang Xiao for technical assistance.

Accepted Manuscript published as ERC-23-0312.R1. Accepted for publication: 11-Apr-2024

References

Aichholzer, F., Klafki, H. W., Ogorek, I., Vogelgsang, J., Wiltfang, J., Scherbaum, N., Weggen, S., & Wirths, O. (2021). Evaluation of cerebrospinal fluid glycoprotein NMB (GPNMB) as a potential biomarker for Alzheimer's disease. *Alzheimers Res Ther*, *13*(1), 94. https://doi.org/10.1186/s13195-021-00828-1

Astrinidis, A., Khare, L., Carsillo, T., Smolarek, T., Au, K. S., Northrup, H., & Henske, E. P. (2000). Mutational analysis of the tuberous sclerosis gene TSC2 in patients with pulmonary lymphangioleiomyomatosis. *J Med Genet*, *37*(1), 55-57. https://doi.org/10.1136/jmg.37.1.55

Carsillo, T., Astrinidis, A., & Henske, E. P. (2000). Mutations in the tuberous sclerosis complex gene TSC2 are a cause of sporadic pulmonary lymphangioleiomyomatosis. *Proc Natl Acad Sci U S A*, *97*(11), 6085-6090. https://doi.org/10.1073/pnas.97.11.6085

Chung, J. S., Tamura, K., Cruz, P. D., Jr., & Ariizumi, K. (2014). DC-HIL-expressing myelomonocytic cells are critical promoters of melanoma growth. *J Invest Dermatol*, *134*(11), 2784-2794. https://doi.org/10.1038/jid.2014.254

Fiorentini, C., Bodei, S., Bedussi, F., Fragni, M., Bonini, S. A., Simeone, C., Zani, D., Berruti, A., Missale, C., Memo, M., Spano, P., & Sigala, S. (2014). GPNMB/OA protein increases the invasiveness of human metastatic prostate cancer cell lines DU145 and PC3 through MMP-2 and MMP-9 activity. *Exp Cell Res*, *323*(1), 100-111. https://doi.org/10.1016/j.yexcr.2014.02.025

Furochi, H., Tamura, S., Mameoka, M., Yamada, C., Ogawa, T., Hirasaka, K., Okumura, Y., Imagawa, T., Oguri, S., Ishidoh, K., Kishi, K., Higashiyama, S., & Nikawa, T. (2007). Osteoactivin fragments produced by ectodomain shedding induce MMP-3 expression via ERK pathway in mouse NIH-3T3 fibroblasts. *FEBS Lett*, *581*(30), 5743-5750. https://doi.org/10.1016/j.febslet.2007.11.036

Glasgow, C. G., Avila, N. A., Lin, J. P., Stylianou, M. P., & Moss, J. (2009). Serum vascular endothelial growth factor-D levels in patients with lymphangioleiomyomatosis reflect lymphatic involvement. *Chest*, *135*(5), 1293-1300. https://doi.org/10.1378/chest.08-1160

Guo, M., Yu, J. J., Perl, A. K., Wikenheiser-Brokamp, K. A., Riccetti, M., Zhang, E. Y., Sudha, P., Adam, M., Potter, A., Kopras, E. J., Giannikou, K., Potter, S. S., Sherman, S., Hammes, S. R., Kwiatkowski, D. J., Whitsett, J. A., McCormack, F. X., & Xu, Y. (2020). Single-Cell Transcriptomic Analysis Identifies a Unique Pulmonary Lymphangioleiomyomatosis Cell. *Am J Respir Crit Care Med*, *202*(10), 1373-1387. https://doi.org/10.1164/rccm.201912-2445OC

Hoashi, T., Sato, S., Yamaguchi, Y., Passeron, T., Tamaki, K., & Hearing, V. J. (2010). Glycoprotein nonmetastatic melanoma protein b, a melanocytic cell marker, is a melanosome-specific and proteolytically released protein. *FASEB J*, *24*(5), 1616-1629. https://doi.org/10.1096/fj.09-151019

Howe, S. R., Gottardis, M. M., Everitt, J. I., Goldsworthy, T. L., Wolf, D. C., & Walker, C. (1995). Rodent model of reproductive tract leiomyomata. Establishment and characterization of tumor-derived cell lines. *Am J Pathol*, *146*(6), 1568-1579. https://www.ncbi.nlm.nih.gov/pubmed/7539981

Huang, Y. H., Chu, P. Y., Chen, J. L., Huang, C. T., Huang, C. C., Tsai, Y. F., Wang, Y. L., Lien, P. J., Tseng, L. M., & Liu, C. Y. (2021). Expression pattern and prognostic impact of glycoprotein non-metastatic B (GPNMB) in triple-negative breast cancer. *Sci Rep*, *11*(1), 12171. https://doi.org/10.1038/s41598-021-91588-3

Huo, D., Liu, Y. Y., Zhang, C., Zeng, L. T., Fan, G. Q., Zhang, L. Q., Pang, J., Wang, Y., Shen, T., Li, X. F., Li, C. B., Zhang, T. M., Cai, J. P., & Cui, J. (2023). Serum glycoprotein non-metastatic melanoma protein B (GPNMB) level as a potential biomarker for diabetes mellitus-related cataract: A cross-sectional study. *Front Endocrinol (Lausanne)*, *14*, 1110337. https://doi.org/10.3389/fendo.2023.1110337

 Accepted Manuscript published as ERC-23-0312.R1. Accepted for publication: 11-Apr-2024

Karbowniczek, M., Astrinidis, A., Balsara, B. R., Testa, J. R., Lium, J. H., Colby, T. V., McCormack, F. X., & Henske, E. P. (2003). Recurrent lymphangiomyomatosis after transplantation: genetic analyses reveal a metastatic mechanism. *Am J Respir Crit Care Med*, *167*(7), 976-982. https://doi.org/10.1164/rccm.200208-969OC

Katayama, A., Nakatsuka, A., Eguchi, J., Murakami, K., Teshigawara, S., Kanzaki, M., Nunoue, T., Hida, K., Wada, N., Yasunaka, T., Ikeda, F., Takaki, A., Yamamoto, K., Kiyonari, H., Makino, H., & Wada, J. (2015). Beneficial impact of Gpnmb and its significance as a biomarker in nonalcoholic steatohepatitis. *Sci Rep*, *5*, 16920. https://doi.org/10.1038/srep16920

Kobayashi, M. (2018). Blocking Monocytic Myeloid-Derived Suppressor Cell Function via Anti-DC-HIL/GPNMB Antibody Restores the In Vitro Integrity of T Cells from Cancer Patients. *AACR*.

Kuan, C. T., Wakiya, K., Dowell, J. M., Herndon, J. E., 2nd, Reardon, D. A., Graner, M. W., Riggins, G. J., Wikstrand, C. J., & Bigner, D. D. (2006). Glycoprotein nonmetastatic melanoma protein B, a potential molecular therapeutic target in patients with glioblastoma multiforme. *Clin Cancer Res*, *12*(7 Pt 1), 1970-1982. https://doi.org/10.1158/1078-0432.CCR-05-2797

Kuhnen, C., Preisler, K., & Muller, K. M. (2001). [Pulmonary lymphangioleiomyomatosis. Morphologic and immunohistochemical findings]. *Pathologe*, *22*(3), 197-204. https://doi.org/10.1007/s002920100462 (Pulmonale Lymphangioleiomyomatose. Morphologische und immunhistochemische Befunde.)

Li, M., Zhu, W. Y., Wang, J., Yang, X. D., Li, W. M., & Wang, G. (2022). Diagnostic performance of VEGF-D for lymphangioleiomyomatosis: a meta-analysis. *J Bras Pneumol*, *48*(1), e20210337. https://doi.org/10.36416/1806-3756/e20210337

Liguori, M., Digifico, E., Vacchini, A., Avigni, R., Colombo, F. S., Borroni, E. M., Farina, F. M., Milanesi, S., Castagna, A., Mannarino, L., Craparotta, I., Marchini, S., Erba, E., Panini, N.,

Tamborini, M., Rimoldi, V., Allavena, P., & Belgiovine, C. (2021). The soluble glycoprotein NMB (GPNMB) produced by macrophages induces cancer stemness and metastasis via CD44 and IL-33. *Cell Mol Immunol*, *18*(3), 711-722. https://doi.org/10.1038/s41423-020-0501-0

Maric, G., Annis, M. G., Dong, Z., Rose, A. A., Ng, S., Perkins, D., MacDonald, P. A., Ouellet, V., Russo, C., & Siegel, P. M. (2015). GPNMB cooperates with neuropilin-1 to promote mammary tumor growth and engages integrin alpha5beta1 for efficient breast cancer metastasis. *Oncogene*, *34*(43), 5494-5504. https://doi.org/10.1038/onc.2015.8

Maric, G., Rose, A. A., Annis, M. G., & Siegel, P. M. (2013). Glycoprotein non-metastatic b (GPNMB): A metastatic mediator and emerging therapeutic target in cancer. *Onco Targets Ther*, *6*, 839-852. https://doi.org/10.2147/OTT.S44906

McCormack, F. X., Gupta, N., Finlay, G. R., Young, L. R., Taveira-DaSilva, A. M., Glasgow, C. G., Steagall, W. K., Johnson, S. R., Sahn, S. A., Ryu, J. H., Strange, C., Seyama, K., Sullivan, E. J., Kotloff, R. M., Downey, G. P., Chapman, J. T., Han, M. K., D'Armiento, J. M., Inoue, Y., . . . Lymphangioleiomyomatosis, A. J. C. o. (2016). Official American Thoracic Society/Japanese Respiratory Society Clinical Practice Guidelines: Lymphangioleiomyomatosis Diagnosis and Management. *Am J Respir Crit Care Med*, *194*(6), 748-761. https://doi.org/10.1164/rccm.201607-1384ST

McCormack, F. X., Inoue, Y., Moss, J., Singer, L. G., Strange, C., Nakata, K., Barker, A. F., Chapman, J. T., Brantly, M. L., Stocks, J. M., Brown, K. K., Lynch, J. P., 3rd, Goldberg, H. J., Young, L. R., Kinder, B. W., Downey, G. P., Sullivan, E. J., Colby, T. V., McKay, R. T., . . . Group, M. T. (2011). Efficacy and safety of sirolimus in lymphangioleiomyomatosis. *N Engl J Med*, *364*(17), 1595-1606. https://doi.org/10.1056/NEJMoa1100391

McCormack, F. X., Travis, W. D., Colby, T. V., Henske, E. P., & Moss, J. (2012). Lymphangioleiomyomatosis: calling it what it is: a low-grade, destructive, metastasizing

Accepted Manuscript published as ERC-23-0312.R1. Accepted for publication: 11-Apr-2024

neoplasm. *Am J Respir Crit Care Med*, *186*(12), 1210-1212. https://doi.org/10.1164/rccm.201205-0848OE

Minor, B. M. N., LeMoine, D., Seger, C., Gibbons, E., Koudouovoh, J., Taya, M., Kurtz, D., Xu, Y., & Hammes, S. R. (2023). Estradiol Augments Tumor-Induced Neutrophil Production to Promote Tumor Cell Actions in Lymphangioleiomyomatosis Models. *Endocrinology*, *164*(6). https://doi.org/10.1210/endocr/bqad061

Murugesan, V., Liu, J., Yang, R., Lin, H., Lischuk, A., Pastores, G., Zhang, X., Chuang, W. L., & Mistry, P. K. (2018). Validating glycoprotein non-metastatic melanoma B (gpNMB, osteoactivin), a new biomarker of Gaucher disease. *Blood Cells Mol Dis*, *68*, 47-53. https://doi.org/10.1016/j.bcmd.2016.12.002

Nijmeh, J., El-Chemaly, S., & Henske, E. P. (2018). Emerging biomarkers of lymphangioleiomyomatosis. *Expert Rev Respir Med*, *12*(2), 95-102. https://doi.org/10.1080/17476348.2018.1409622

Oyewumi, M. O., Manickavasagam, D., Novak, K., Wehrung, D., Paulic, N., Moussa, F. M., Sondag, G. R., & Safadi, F. F. (2016). Osteoactivin (GPNMB) ectodomain protein promotes growth and invasive behavior of human lung cancer cells. *Oncotarget*, *7*(12), 13932-13944. https://doi.org/10.18632/oncotarget.7323

Palisoc, P. J., Vaikutis, L., Gurrea-Rubio, M., Model, E. N., O'Mara M, M., Ory, S., Vichaikul, S., Khanna, D., Tsou, P. S., & Sawalha, A. H. (2022). Functional Characterization of Glycoprotein Nonmetastatic Melanoma Protein B in Scleroderma Fibrosis. *Front Immunol*, *13*, 814533. https://doi.org/10.3389/fimmu.2022.814533

Pollack, V. A., Alvarez, E., Tse, K. F., Torgov, M. Y., Xie, S., Shenoy, S. G., MacDougall, J. R., Arrol, S., Zhong, H., Gerwien, R. W., Hahne, W. F., Senter, P. D., Jeffers, M. E., Lichenstein, H. S., & LaRochelle, W. J. (2007). Treatment parameters modulating regression of human melanoma xenografts by an antibody-drug conjugate (CR011-

vcMMAE) targeting GPNMB. *Cancer Chemother Pharmacol*, *60*(3), 423-435. https://doi.org/10.1007/s00280-007-0490-z

Prizant, H., & Hammes, S. R. (2016). Minireview: Lymphangioleiomyomatosis (LAM): The "Other" Steroid-Sensitive Cancer. *Endocrinology*, *157*(9), 3374-3383. https://doi.org/10.1210/en.2016-1395

Prizant, H., Taya, M., Lerman, I., Light, A., Sen, A., Mitra, S., Foster, T. H., & Hammes, S. R. (2016). Estrogen maintains myometrial tumors in a lymphangioleiomyomatosis model. *Endocr Relat Cancer*, *23*(4), 265-280. https://doi.org/10.1530/ERC-15-0505

Qian, X., Mills, E., Torgov, M., LaRochelle, W. J., & Jeffers, M. (2008). Pharmacologically enhanced expression of GPNMB increases the sensitivity of melanoma cells to the CR011-vcMMAE antibody-drug conjugate. *Mol Oncol*, *2*(1), 81-93. https://doi.org/10.1016/j.molonc.2008.02.002

Rich, J. N., Shi, Q., Hjelmeland, M., Cummings, T. J., Kuan, C. T., Bigner, D. D., Counter, C. M., & Wang, X. F. (2003). Bone-related genes expressed in advanced malignancies induce invasion and metastasis in a genetically defined human cancer model. *J Biol Chem*, *278*(18), 15951-15957. https://doi.org/10.1074/jbc.M211498200

Ripoll, V. M., Irvine, K. M., Ravasi, T., Sweet, M. J., & Hume, D. A. (2007). Gpnmb is induced in macrophages by IFN-gamma and lipopolysaccharide and acts as a feedback regulator of proinflammatory responses. *J Immunol*, *178*(10), 6557-6566. https://doi.org/10.4049/jimmunol.178.10.6557

Rose, A. A., Annis, M. G., Dong, Z., Pepin, F., Hallett, M., Park, M., & Siegel, P. M. (2010). ADAM10 releases a soluble form of the GPNMB/Osteoactivin extracellular domain with angiogenic properties. *PLoS One*, *5*(8), e12093. https://doi.org/10.1371/journal.pone.0012093

Rose, A. A., Grosset, A. A., Dong, Z., Russo, C., Macdonald, P. A., Bertos, N. R., St-Pierre, Y., Simantov, R., Hallett, M., Park, M., Gaboury, L., & Siegel, P. M. (2010). Glycoprotein

Accepted Manuscript published as ERC-23-0312.R1. Accepted for publication: 11-Apr-2024

nonmetastatic B is an independent prognostic indicator of recurrence and a novel therapeutic target in breast cancer. *Clin Cancer Res*, *16*(7), 2147-2156. https://doi.org/10.1158/1078-0432.CCR-09-1611

Rose, A. A., Pepin, F., Russo, C., Abou Khalil, J. E., Hallett, M., & Siegel, P. M. (2007). Osteoactivin promotes breast cancer metastasis to bone. *Mol Cancer Res*, *5*(10), 1001-1014. https://doi.org/10.1158/1541-7786.MCR-07-0119

Rose, A. A. N., Biondini, M., Curiel, R., & Siegel, P. M. (2017). Targeting GPNMB with glembatumumab vedotin: Current developments and future opportunities for the treatment of cancer. *Pharmacol Ther*, *179*, 127-141. https://doi.org/10.1016/j.pharmthera.2017.05.010

Ryu, J. H., Moss, J., Beck, G. J., Lee, J. C., Brown, K. K., Chapman, J. T., Finlay, G. A., Olson, E. J., Ruoss, S. J., Maurer, J. R., Raffin, T. A., Peavy, H. H., McCarthy, K., Taveira-Dasilva, A., McCormack, F. X., Avila, N. A., Decastro, R. M., Jacobs, S. S., Stylianou, M., . . . Group, N. L. R. (2006). The NHLBI lymphangioleiomyomatosis registry: characteristics of 230 patients at enrollment. *Am J Respir Crit Care Med*, *173*(1), 105-111. https://doi.org/10.1164/rccm.200409-1298OC

Saha, N., Robev, D., Himanen, J. P., & Nikolov, D. B. (2019). ADAM proteases: Emerging role and targeting of the non-catalytic domains. *Cancer Lett*, *467*, 50-57. https://doi.org/10.1016/j.canlet.2019.10.003

Strizheva, G. D., Carsillo, T., Kruger, W. D., Sullivan, E. J., Ryu, J. H., & Henske, E. P. (2001). The spectrum of mutations in TSC1 and TSC2 in women with tuberous sclerosis and lymphangiomyomatosis. *Am J Respir Crit Care Med*, *163*(1), 253-258. https://doi.org/10.1164/ajrccm.163.1.2005004

Taghizadeh, L. A., King, C. J., Nascene, D. R., Gupta, A. O., Orchard, P. J., Higgins, L., Markowski, T. W., Nolan, E. E., Furcich, J. W., & Lund, T. C. (2022). Glycoprotein nonmetastatic melanoma protein B (GNMPB) as a novel biomarker for cerebral

adrenoleukodystrophy. *Sci Rep*, *12*(1), 7985. https://doi.org/10.1038/s41598-022-11552-7

Taveira-DaSilva, A. M., Johnson, S. R., Julien-Williams, P., Johnson, J., Stylianou, M., & Moss, J. (2020). Pregnancy in lymphangioleiomyomatosis: clinical and lung function outcomes in two national cohorts. *Thorax*, *75*(10), 904-907. https://doi.org/10.1136/thoraxjnl-2020-214987

Taya, M., & Hammes, S. R. (2018). Glycoprotein Non-Metastatic Melanoma Protein B (GPNMB) and Cancer: A Novel Potential Therapeutic Target. *Steroids*, *133*, 102-107. https://doi.org/10.1016/j.steroids.2017.10.013

Tomihari, M., Chung, J. S., Akiyoshi, H., Cruz, P. D., Jr., & Ariizumi, K. (2010). DC-HIL/glycoprotein Nmb promotes growth of melanoma in mice by inhibiting the activation of tumor-reactive T cells. *Cancer Res*, *70*(14), 5778-5787. https://doi.org/10.1158/0008-5472.CAN-09-2538

Torres, C., Linares, A., Alejandre, M. J., Palomino-Morales, R., Martin, M., Delgado, J. R., Martinez, J., & Perales, S. (2015). The potential role of the glycoprotein osteoactivin/glycoprotein nonmetastatic melanoma protein B in pancreatic cancer. *Pancreas*, *44*(2), 302-310. https://doi.org/10.1097/MPA.0000000000000250

Tse, K. F., Jeffers, M., Pollack, V. A., McCabe, D. A., Shadish, M. L., Khramtsov, N. V., Hackett, C. S., Shenoy, S. G., Kuang, B., Boldog, F. L., MacDougall, J. R., Rastelli, L., Herrmann, J., Gallo, M., Gazit-Bornstein, G., Senter, P. D., Meyer, D. L., Lichenstein, H. S., & LaRochelle, W. J. (2006). CR011, a fully human monoclonal antibody-auristatin E conjugate, for the treatment of melanoma. *Clin Cancer Res*, *12*(4), 1373-1382. https://doi.org/10.1158/1078-0432.CCR-05-2018

Vaklavas, C., & Forero, A. (2014). Management of metastatic breast cancer with second-generation antibody-drug conjugates: focus on glembatumumab vedotin (CDX-011, CR011-vcMMAE). *BioDrugs*, *28*(3), 253-263. https://doi.org/10.1007/s40259-014-0085-2

Accepted Manuscript published as ERC-23-0312.R1. Accepted for publication: 11-Apr-2024

Wang, J., Zhang, X., Long, M., Yuan, M., Yin, J., Luo, W., Wang, S., Cai, Y., Jiang, W., & Chao, J. (2023). Macrophage-derived GPNMB trapped by fibrotic extracellular matrix promotes pulmonary fibrosis. *Commun Biol*, *6*(1), 136. https://doi.org/10.1038/s42003-022-04333-5

Weterman, M. A., Ajubi, N., van Dinter, I. M., Degen, W. G., van Muijen, G. N., Ruitter, D. J., & Bloemers, H. P. (1995). nmb, a novel gene, is expressed in low-metastatic human melanoma cell lines and xenografts. *Int J Cancer*, *60*(1), 73-81. https://doi.org/10.1002/ijc.2910600111

Young, L., Lee, H. S., Inoue, Y., Moss, J., Singer, L. G., Strange, C., Nakata, K., Barker, A. F., Chapman, J. T., Brantly, M. L., Stocks, J. M., Brown, K. K., Lynch, J. P., 3rd, Goldberg, H. J., Downey, G. P., Swigris, J. J., Taveira-DaSilva, A. M., Krischer, J. P., Trapnell, B. C., . . . Group, M. T. (2013). Serum VEGF-D a concentration as a biomarker of lymphangioleiomyomatosis severity and treatment response: a prospective analysis of the Multicenter International Lymphangioleiomyomatosis Efficacy of Sirolimus (MILES) trial. *Lancet Respir Med*, *1*(6), 445-452. https://doi.org/10.1016/S2213-2600(13)70090-0

Zhang, Y. X., Qin, C. P., Zhang, X. Q., Wang, Q. R., Zhao, C. B., Yuan, Y. Q., & Yang, J. G. (2017). Knocking down glycoprotein nonmetastatic melanoma protein B suppresses the proliferation, migration, and invasion in bladder cancer cells. *Tumour Biol*, *39*(4), 1010428317699119. https://doi.org/10.1177/1010428317699119

Figure Legends

Figure 1. **GPNMB knockdown decreases TSC2-null rat ELT3 cell invasion, but not proliferation or migration. A.** Representative western blot showing the knockdown efficiency of GPNMB in ELT3 cells treated with non-specific (NSP) siRNA or *GPNMB* specific siRNA. **B.** Relative absorbance for the BRDU proliferation assay. Cells were plated for 48 hours and then BRDU was added for 24 hours. Paired t-test for 4 experiments (5 replicates per experiment) (ns=not significant). **C.** Cell proliferation was measured by counting cells plated on collagen coated plates (9.87 μg/cm^2 of collagen per well) with the Celigo image cytometer at 24, 48, and 72 hours after plating and growth rate was compared to 24 hours for NSP and *GPNMB*-specific siRNA transfected cells respectively. **D.** Relative absorbance for the MTT cell metabolic rate assay. Cells were plated for 72 hours before the addition of MTT. n=4 (5 replicates per experiment) Paired t-test (**p<0.01). **E.** Representative images of transwell migration assay. **F.** Cell migration relative to NSP, n=5 (2 replicates per experiment with 5 images averaged per transwell). Paired t-test. **G.** Representative images of transwell invasion assay. **H.** Cell invasion relative to NSP, n=4 (2 replicates per experiment with 5 images averaged per transwell). Paired t-test. (*p<0.05).

Figure 2. **GPNMB-null ELT3-Luc cell xenografts grow slower relative to controls in SCID-NOD mice. A.** Western blot analysis of protein from tumors demonstrates the presence of GPNMB expression in four representative control xenografts at the end of the experiment (10 weeks post injection) and the absence of GPNMB expression in four representative CRISPR-mediated GPNMB knockout (KO) xenografts at the end of the experiment, with GAPDH as a loading control. **B.** Representative immunofluorescence images (20x magnification) of one control clone xenograft (top) and one CRISPR-mediated GPNMB KO xenograft (bottom). DAPI-blue, GPNMB-green. **C.** The average tumor volume over time for control clones and CRISPR clones

 Accepted Manuscript published as ERC-23-0312.R1. Accepted for publication: 11-Apr-2024

Tumor volume was calculated using the formula $(L*(W)^2)/2$. **D.** The final tumor weight in grams of controls and GPNMB KO (n= 18 control tumors, n= 11 GPNMB KO tumors). Statistical analysis for C and D was performed using unpaired two-tailed t-tests. (*p<0.05, **p<0.01). **E.** Representative images of blue Trichrome collagen staining in one control and one GPNMB KO tumor (same tumors from B). **F.** Quantification of the positive pixels/area of tumor in mm^2 using Aperio ImageScope collagen staining analysis add-in. n=3 tumors (all different clones) per group. Statistical analysis was performed using an unpaired two-tailed t-test. (**p<0.01).

Figure 3. **Serum starvation increases GPNMB expression in a transcription- and mTORC1-dependent manner in ELT3 cells. A.** Fold change of *Gpnmb* relative to *Gapdh* mRNA determined by RT-qPCR for ELT3 cells in complete media with serum, serum starved for 24 hours, and then serum starved for 24 hours with FBS added back for 10, 30, minutes, 1 hour, or 24 hours (indicated as “Time” under the x-axis). **B.** ELT3 cells were treated with DMSO (control) or 5 μM Actinomycin D (ActD) under complete media or starvation conditions for 24 hours. Fold change of *Gpnmb* relative to *Gapdh* mRNA was determined by RT-qPCR setting the complete media with DMSO (no ActD) condition to 1. **C.** ELT3 cells were treated with ethanol (control) or 20nM Rapamycin (Rapa) for 24 hours in complete media or serum-free media. Fold-change of *Gpnmb* relative to *Gapdh* mRNA was determined by RT-qPCR, setting the complete media with ethanol (no rapamycin) condition to 1. **D.** Representative GPNMB and GAPDH western blot (one experiment of three with similar results) using the same conditions from (A). **E.** Representative GPNMB and GAPDH western blot (one experiment of three with similar results) of the same sample conditions from (B). **F.** Representative western blot of the samples quantified in G. S6=phosphorylated S6 protein, which reflects mTORC1 activation. tS6=total S6 protein. **G.** Quantification of GPNMB relative to GAPDH protein expression in (F), using ImageJ, setting the complete media with ethanol condition to 1 (n= 3 experiments). All statistics used One-way ANOVA (*p<0.05, **p<0.01 ***p<0.001, ****p<0.0001). **H.** pS6/tS6 western blot band intensities

normalized to complete media with vehicle (+serum, -Rapa). (same samples as G) Paired t-test, ns=non-significant.

Figure 4. **Adam10 and 17 mediate GPNMB ectodomain shedding in human TSC2-null 621-101 cells. A.** *ADAM10* mRNA knockdown efficiency using siRNA determined by RT-qPCR. The average knockdown efficiency was 85% for 6 experiments. Paired t-tests (****p<0.0001, ns= non-significant). AD10=ADAM10; AD17=ADAM17. **B.** *ADAM17* mRNA mRNA knockdown efficiency using siRNA determined by RT-qPCR. The average knockdown efficiency was 68% for 6 experiments. Paired t-tests (****p<0.0001, ns= non-significant). **C.** Western blot shows GPNMB protein levels in lysate and media samples from cells treated with non-specific (NSP), Adam10, or Adam17 siRNA. Data from one experiment representative of 6 experiments. **D.** ImageJ was used to quantify band intensity of the media samples relative to the lysate. Paired t-tests (***p<0.001, * p<0.05). **E.** Representative western blot image of GPNMB levels in lysate and media from cells treated with ADAM10 or ADAM17 inhibitors (n=3 experiments total). Vehicle (0μM) is DMSO, GIX (15 μM) is an ADAM10 selective inhibitor, TAPI (20 μM) is an ADAM17 selective inhibitor. **F.** Representative western blot of GPNMB expression from 1 experiment out of 3 where cells were treated with vehicle or a combination of 15 μM GIX and 20 μM TAPI. **G.** ImageJ was used to quantify band intensity of the media samples relative to the lysate for experiments in E and F. Paired t-tests (* p<0.05).

Figure 5. **Identification of the cleavage site of GPNMB. A.** Schematic of the basic structure of human GPNMB demonstrating the identified cleavage site of the GPNMB ectodomain (VRR). Figure made in Biorender. VRR- 3 amino acids (9 base pairs) were deleted through site-directed mutagenesis. **B.** Flow cytometry histogram overlay of cell surface expression of GPNMB in knockout ELT3-Luc cells transfected with no DNA mock control (CTRL, red), cDNA encoding human GPNMB (WT, blue), or cDNA encoding human GPNMB with a deleted VRR sequence

 Accepted Manuscript published as ERC-23-0312.R1. Accepted for publication: 11-Apr-2024

(MUT, orange). Data from one experiment representative of 2 experiments. **C.** Western blot of cell lysate and media for GPNMB and GAPDH from GPNMB knockout (KO) ELT3-Luc cells transfected with no DNA mock control, cDNA encoding human GPNMB, or cDNA encoding human GPNMB with a deleted VRR sequence (image representative of 3 separate experiments). **D.** ELISA to detect the human GPNMB ectodomain from the media from the experiment in (C). n= 3. Unpaired t-test (* $p<0.05$). **E.** Western Blot of cell lysate for GPNMB and GAPDH for stable clones expressing wild-type human GPNMB (n=4) or mutant GPNMB with a deleted VRR sequence (n=2). **F.** ELISA to detect the human GPNMB ectodomain from stable clones expressing WT GPNMB or the mutant GPNMB. n= 4 WT and n= 2 mutant. Unpaired t-test (* $p<0.05$).

Figure 6. **ELT3-Luc cells stably expressing mutant non-cleavable human GPNMB grow slower relative to cells stably expressing wild-type human GPNMB in xenografts in SCID-NOD mice.** One of the CRISPR knockout GPNMB clones was used to create clones that either re-expressed wild-type GPNMB or the non-cleavable mutant form of GPNMB. **A.** The average tumor volume over time for 2 clones expressing wild-type GPNMB or two clones expressing mutant GPNMB. GP= GPNMB, MUT= mutant. n= 16 GP tumors, n=9 MUT tumors. Tumor volume was calculated using the formula $(L*(W)^2)/2$. **B.** Final tumor weight (g). Statistics for A and B used unpaired two-tailed t-tests (* $p<0.05$). **C.** GPNMB ectodomain levels in serum detected by ELISA. **D.** Representative western blot of GPNMB and GAPDH for non-specific (NSP) and GPNMB knockdown with siRNA. E. Knockdown efficiency calculated using ImageJ relative intensities of GPNMB/GAPDH western blot bands. n=3, ***$p<0.001$. **F.** Representative images of transwell invasion assay. **G.** Cell invasion relative to NSP, n=3 (2 replicates per experiment with 5 images averaged per transwell). Paired t-test. ns=non-significant.

Figure 7. **GPNMB ectodomain levels are increased in the serum of human patients with LAM compared to healthy controls and decrease with sirolimus treatment. A.** Human GPNMB ELISA kit was used with 5ul of serum (n=30 control, n=30 LAM). *p<0.05 Wilcoxon's Test. **B.** Paired serum samples from 10 patients before and 3 months after Sirolimus treatment. Paired t-test. p= 0.0388. **C.** Serum GPNMB (pg/mL) for all MILES trial patients in the Sirolimus treated group. n= 44 (0 months), 36 (6 months), 32 (12 months), 17 (24 months). Treatment ceased at 12 months. Mixed effects analysis (**p<0.01, ****p<0.0001) **D.** GPNMB (pg/mL) for all MILES trial patients in the Placebo treated group. Mixed effects analysis (*p<0.05, **p<0.01). **E.** Average serum GPNMB levels by ELISA for all patients in (C) and (D). Treatment was stopped at 12 months as indicated by the arrow. Multiple unpaired t-tests (***p<0.001). Patient numbers for each group at the indicated time points are indicated below E.

Accepted Manuscript published as ERC-23-0312.R1. Accepted for publication: 11-Apr-2024

Figure 1

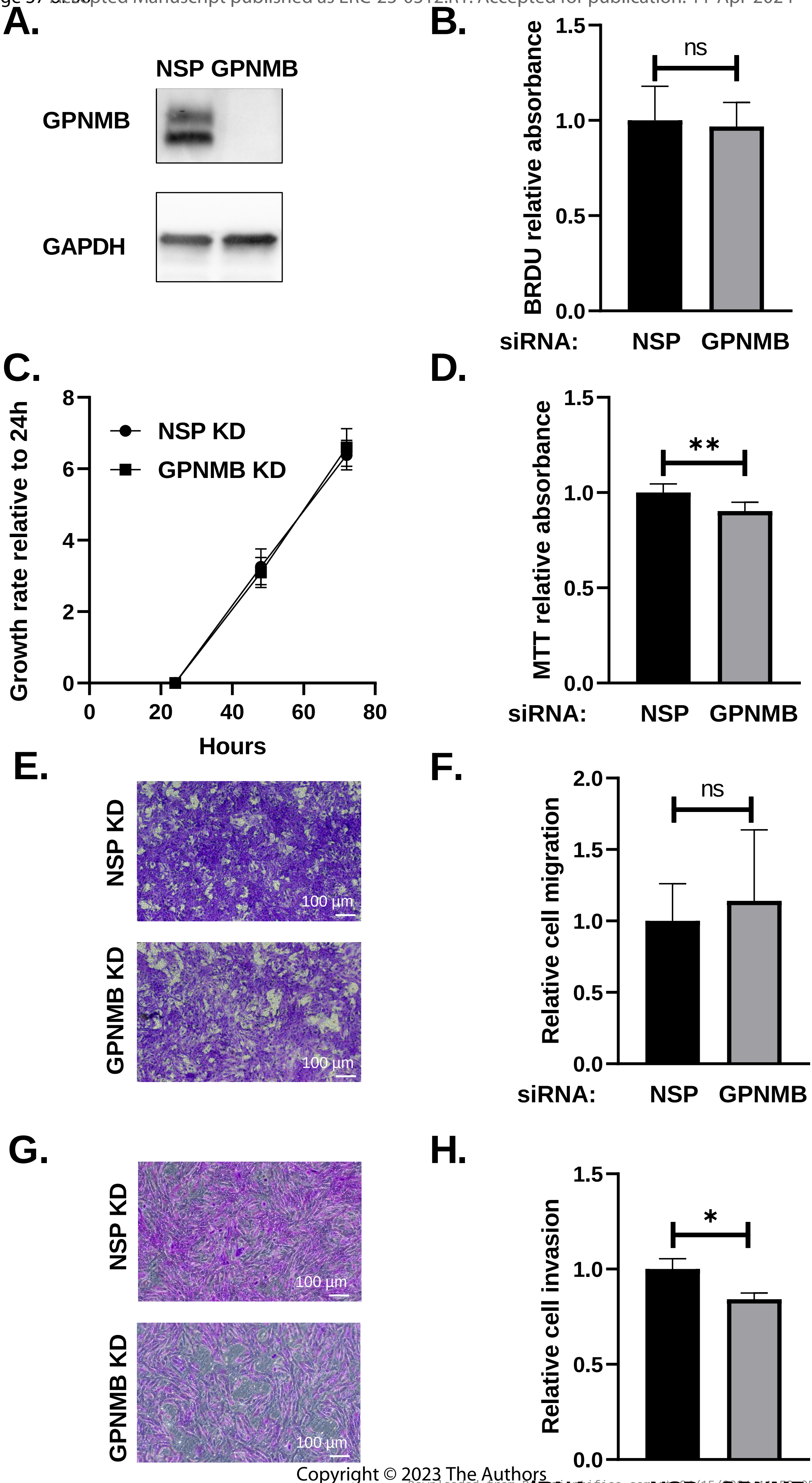

Accepted Manuscript published as ERC-23-0312.R1. Accepted for publication: 11-Apr-2024

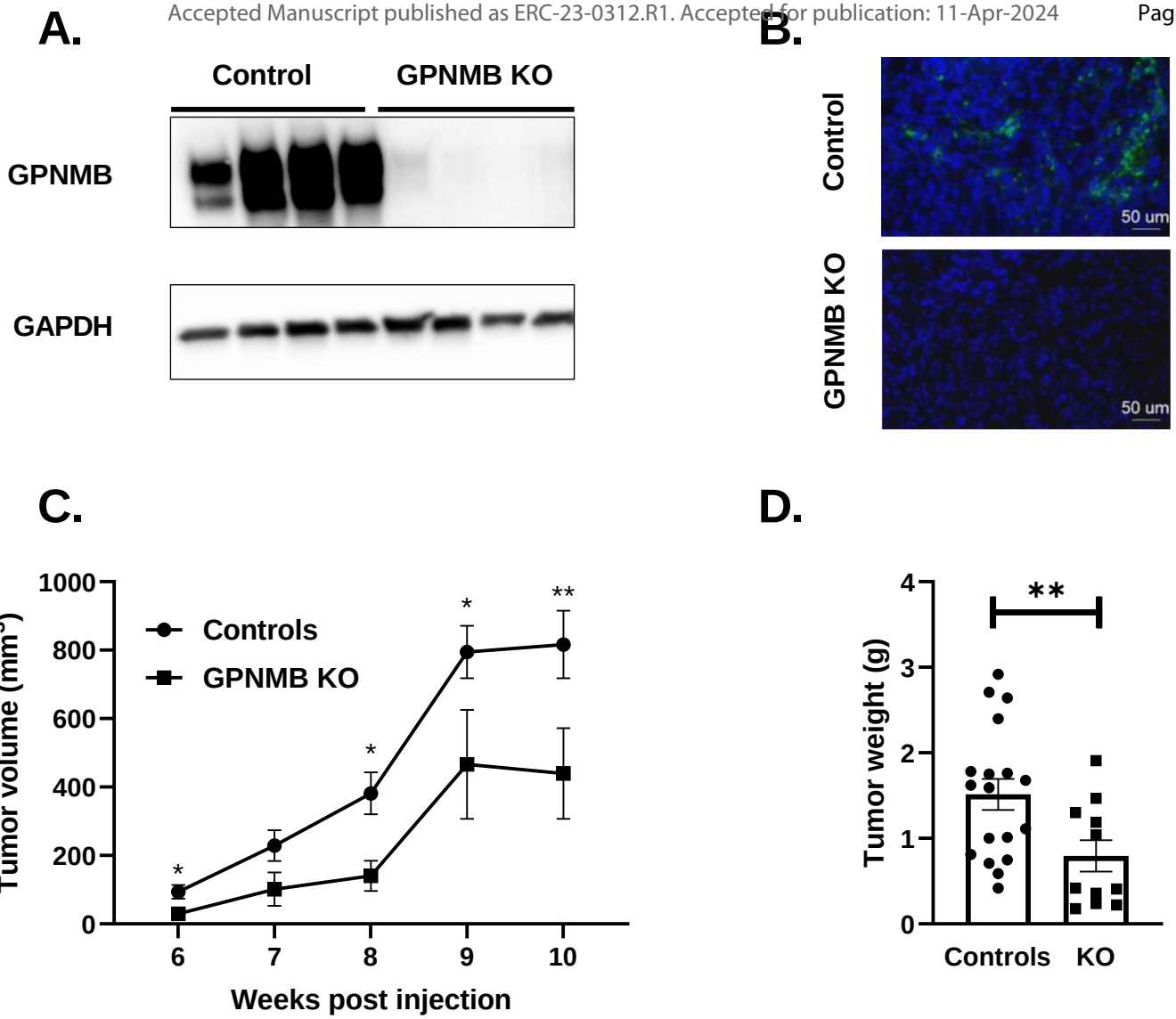

Accepted Manuscript published as ERC-23-0312.R1. Accepted for publication: 11-Apr-2024

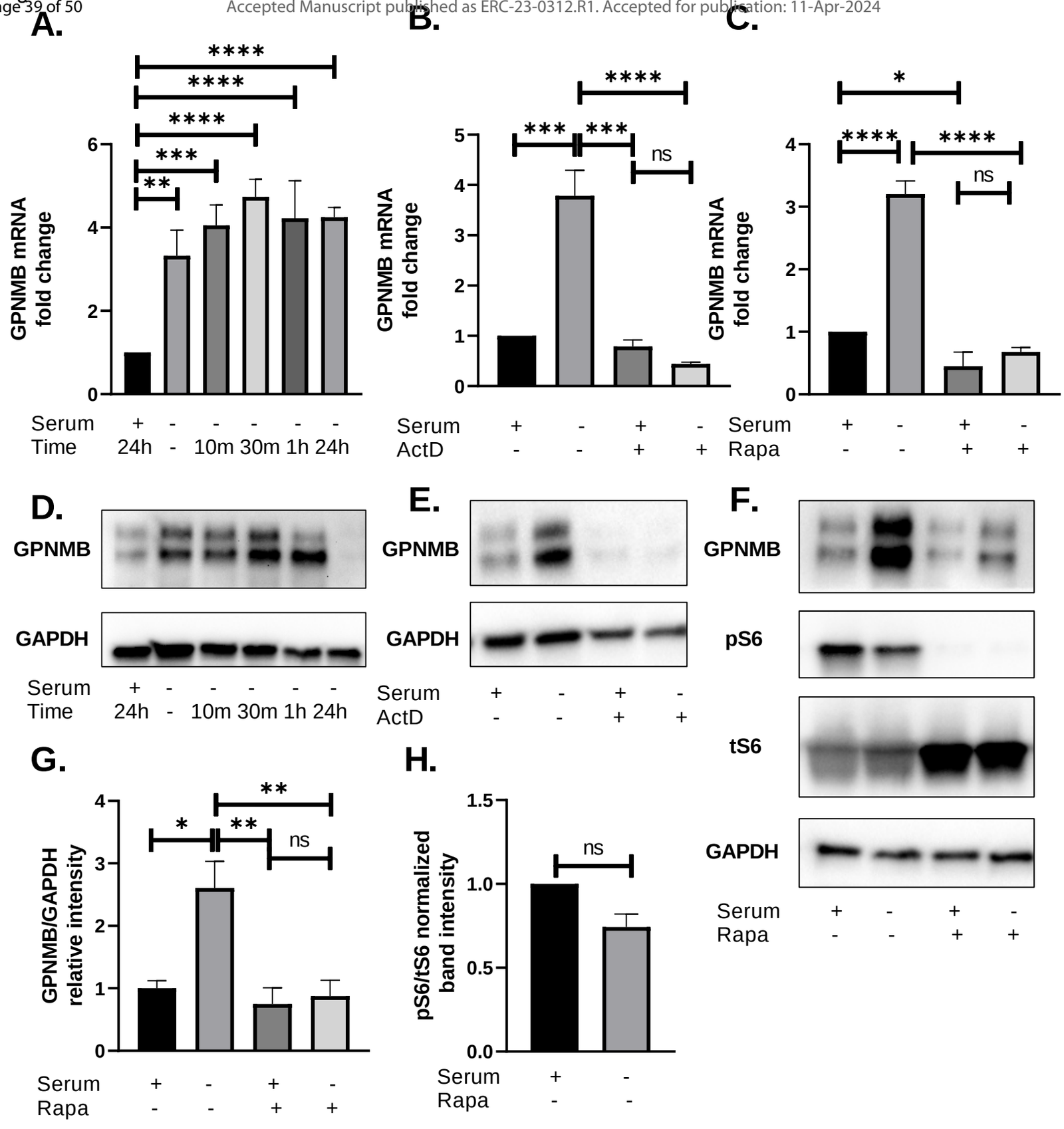

Accepted Manuscript published as ERC-23-0312.R1. Accepted for publication: 11-Apr-2024

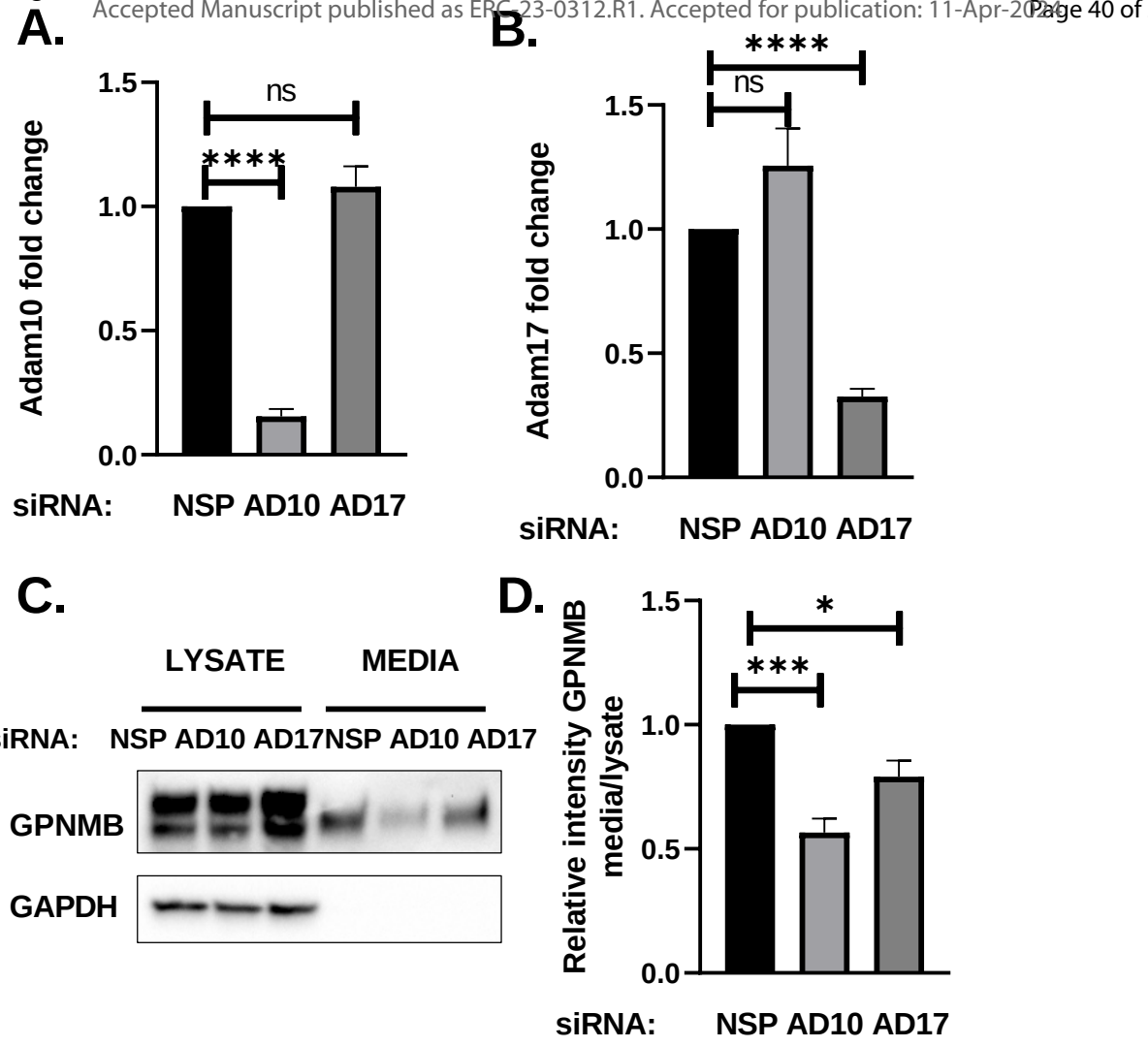

Accepted Manuscript published as ERC-23-0312.R1. Accepted for publication: 11-Apr-2024

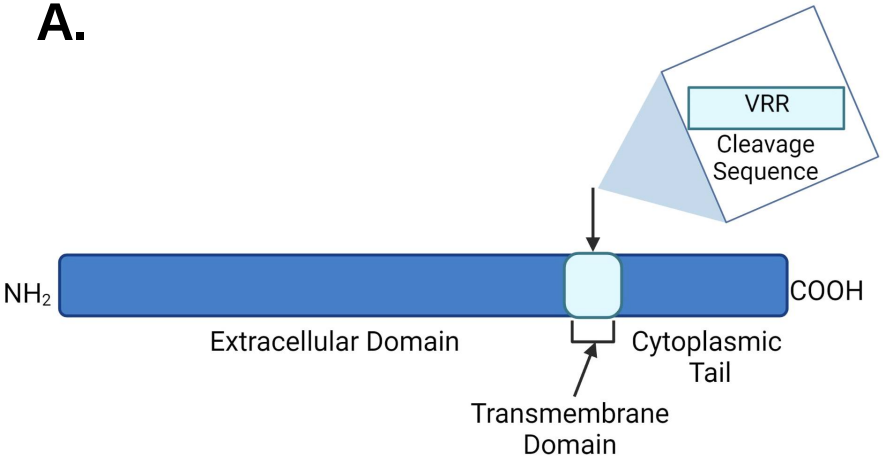

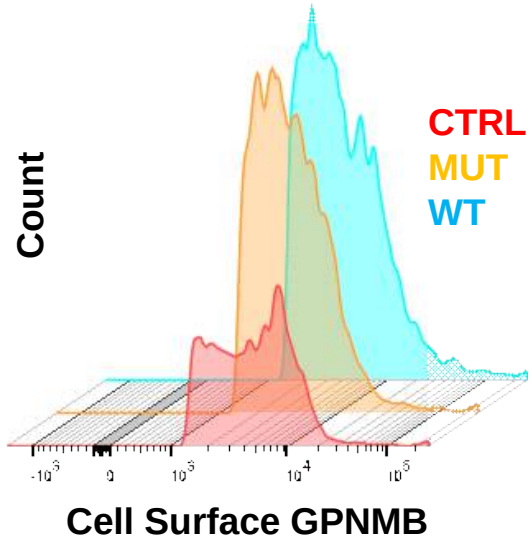

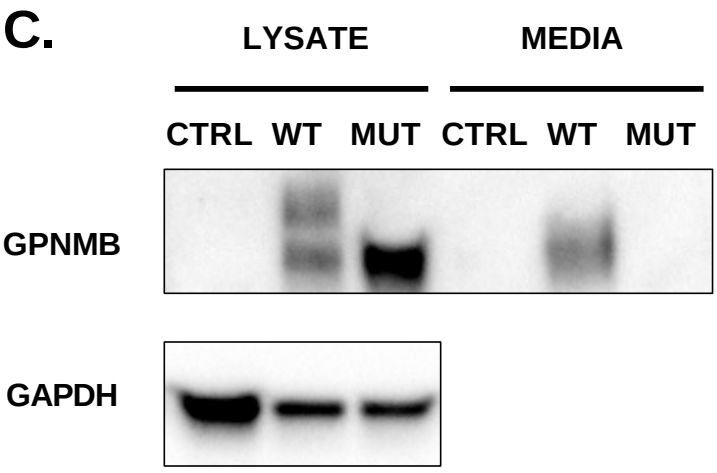

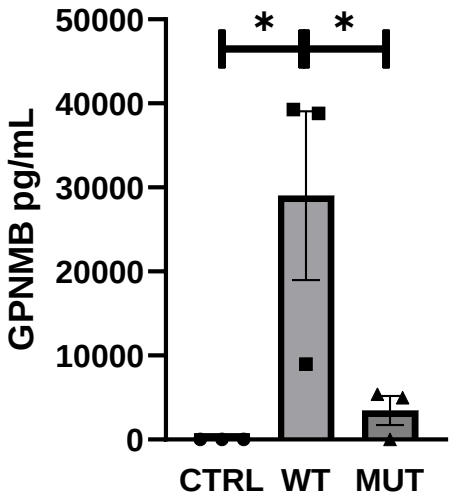

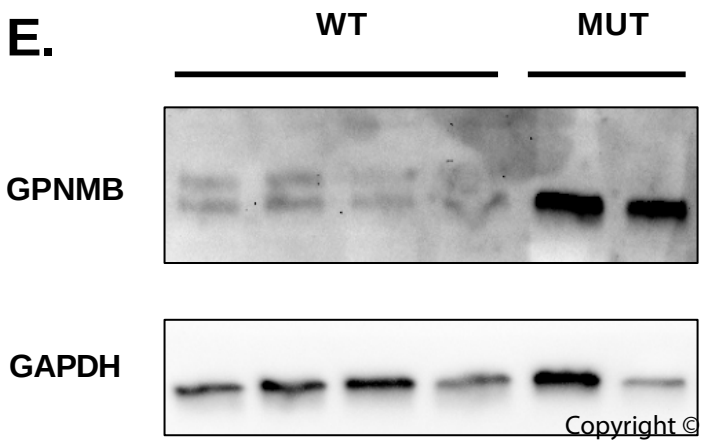

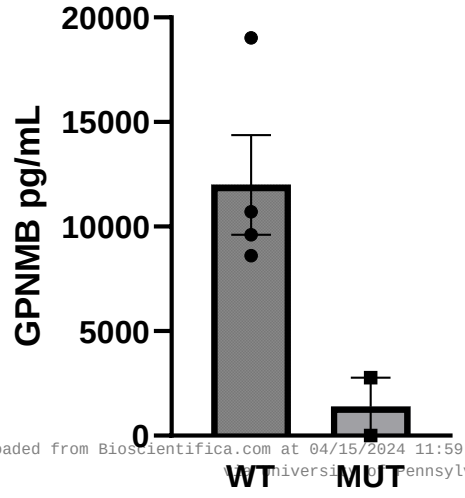

Accepted Manuscript published as ERC-23-0312.R1. Accepted for publication 11-Apr-2024

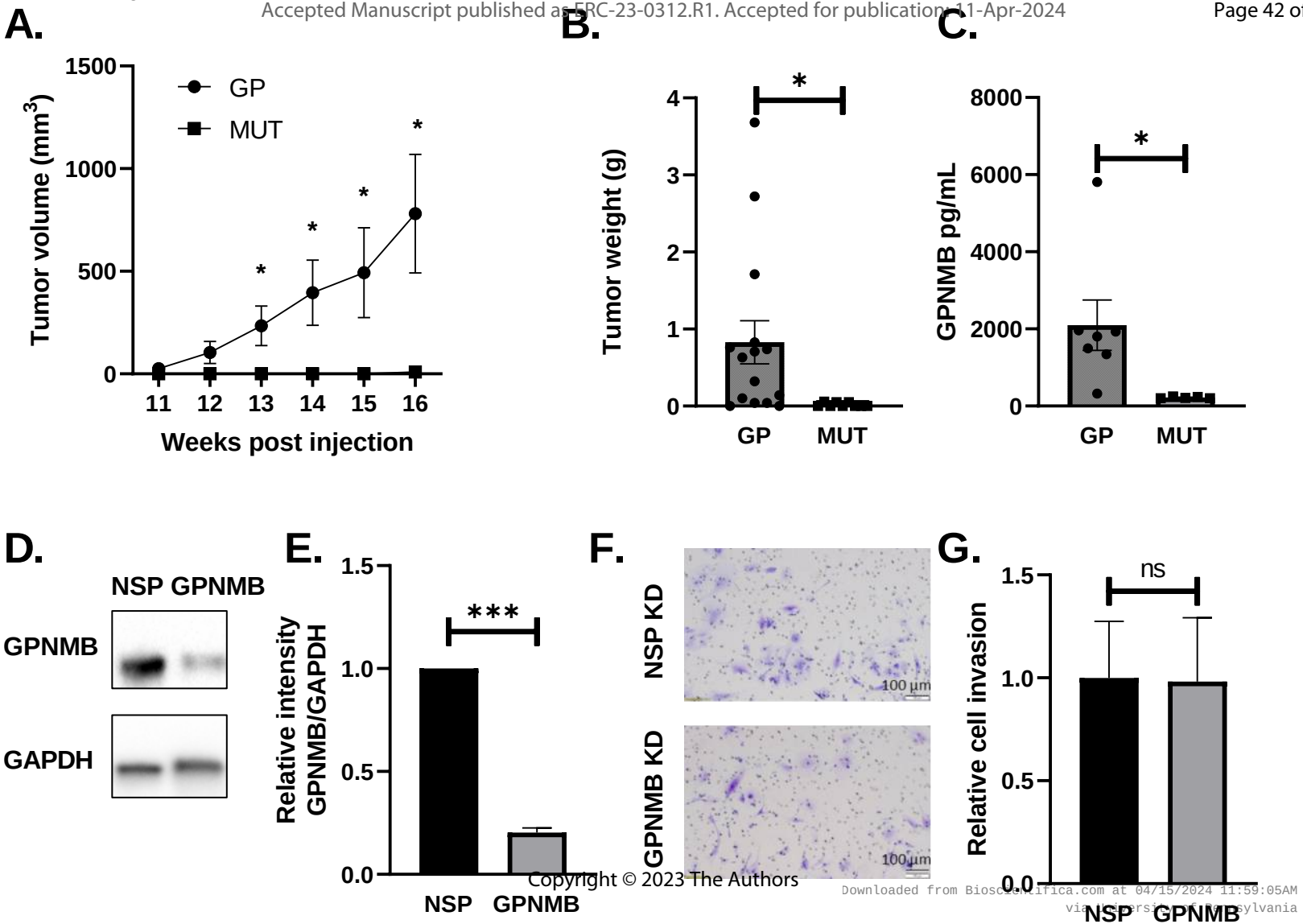

Accepted Manuscript published as ERC-23-0312.R1. Accepted for publication: 11-Apr-2024

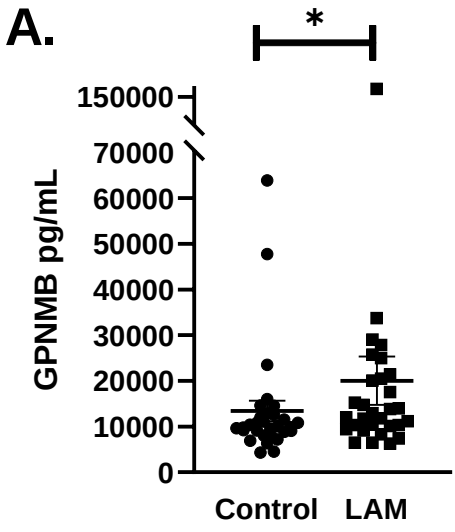

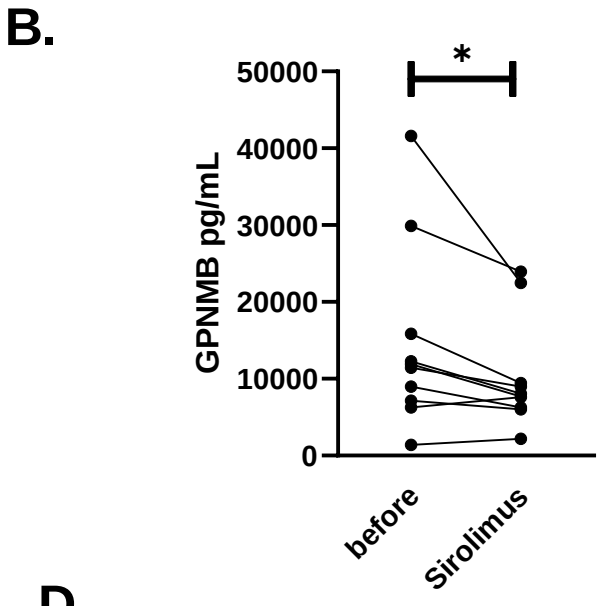

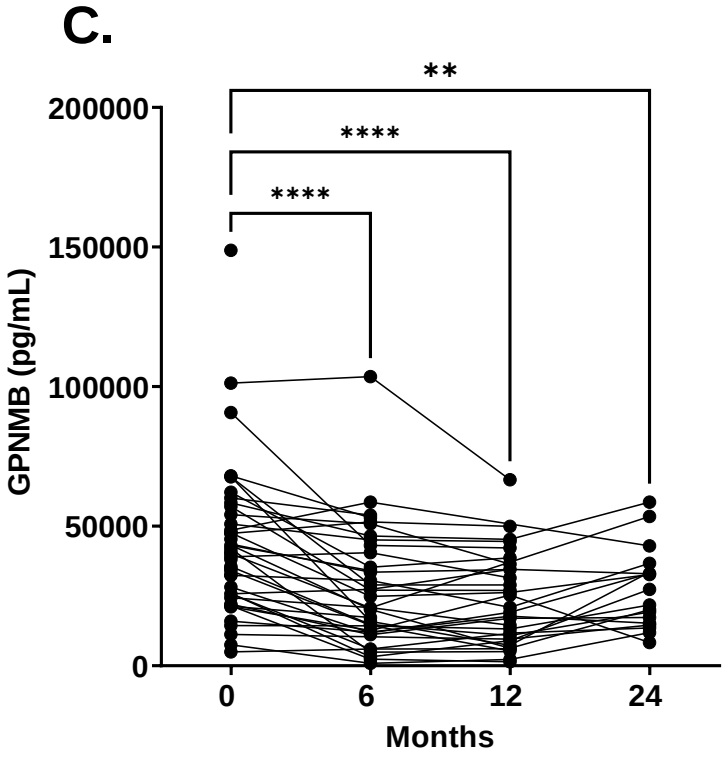

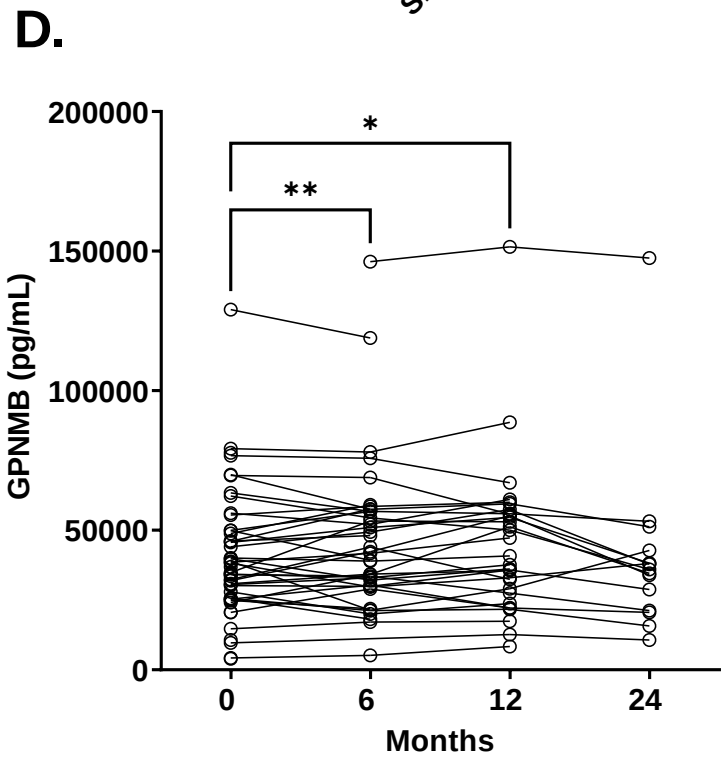

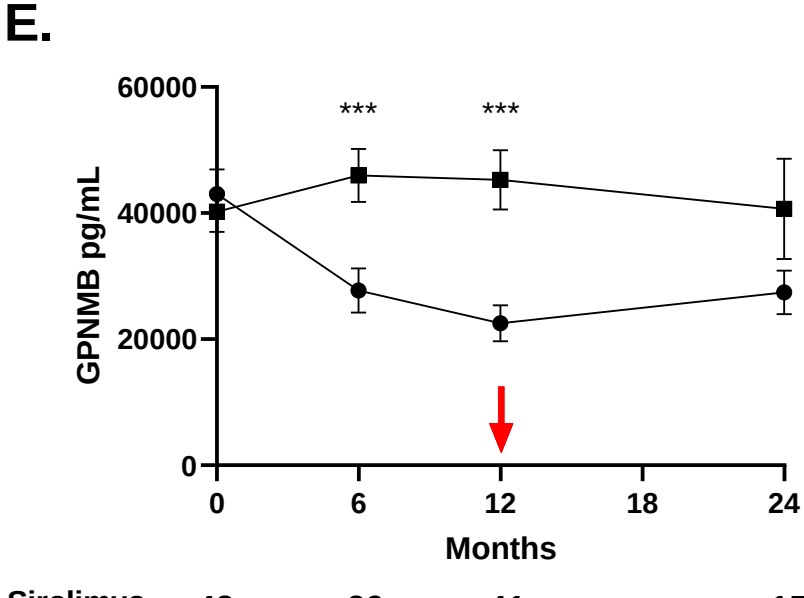

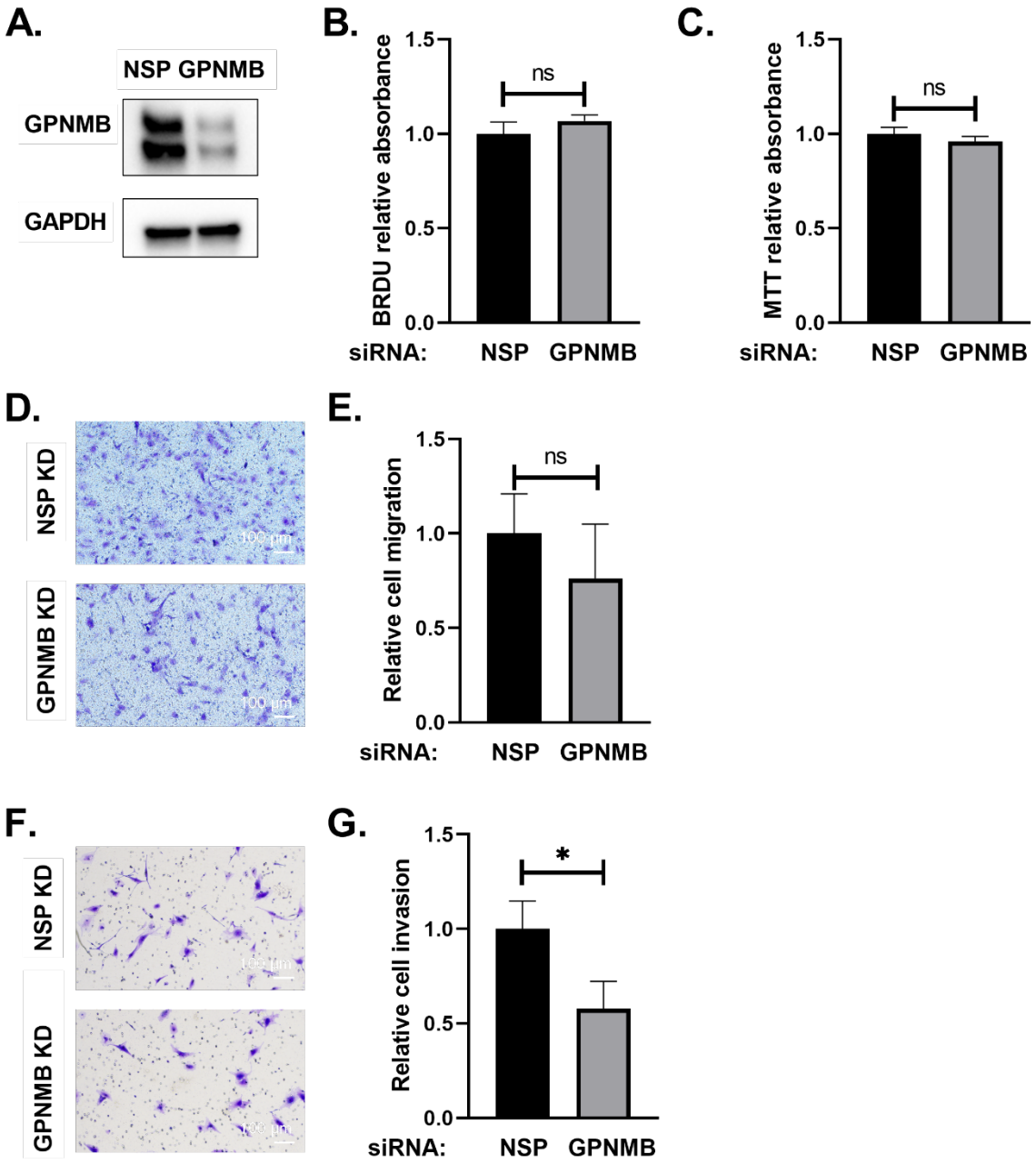

Supplemental Figure 1. **siRNA-mediated GPNMB knockdown reduces invasion, but not proliferation of migration, of mouse TSC2-null mouse LTM3 cells. A.** Representative western blot showing the knockdown efficiency of GPNMB in LTM3 cells treated with non-specific (NSP) siRNA or *GPNMB* specific siRNA. **B.** Relative absorbance for the BRDU proliferation assay. Paired t-test for 4 experiments (5 replicates per experiment). ns=not significant. **C.** Relative absorbance for the MTT cell metabolic rate assay. Cells were plated for 72 hours before the addition of MTT. n=7 (5 replicates per experiment). Paired t-test. **D.** Representative images of transwell migration assay. **E.** Cell migration relative to NSP, n=3 (2 replicates per experiment with 5 images averaged per transwell). Paired t-test. **F.** Representative images of transwell invasion assay. **G.** Cell invasion relative to NSP, n=5 (2 replicates per experiment with 5 images averaged per transwell). Paired t-test, (*p<0.05).

Accepted Manuscript published as ERC-23-0312.R1. Accepted for publication: 11-Apr-2024

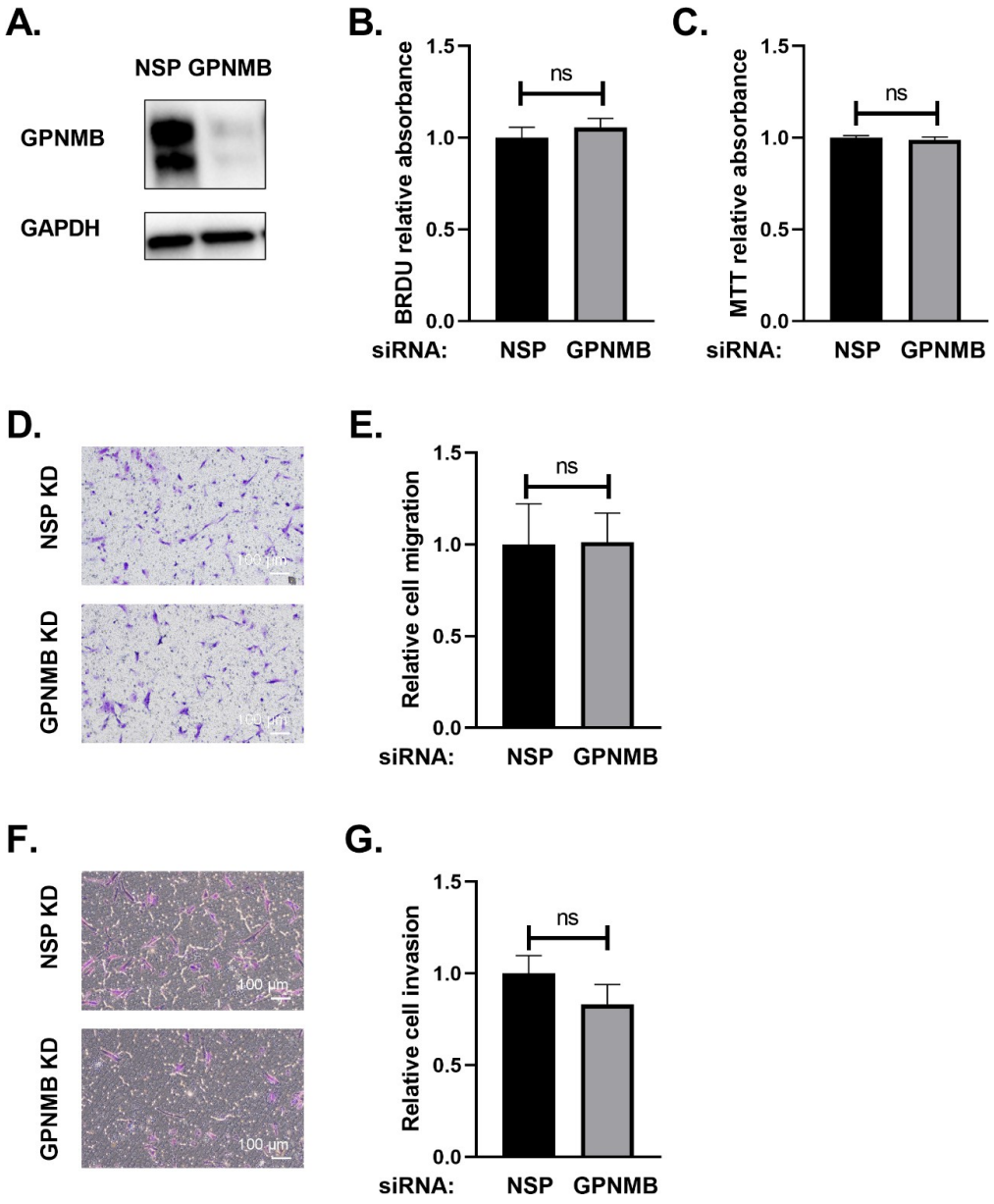

Supplemental Figure 2. **siRNA-mediated GPNMB knockdown has minimal effects *in vitro* on human TSC2-null 621-101 cells. A.** Representative western blot showing the knockdown efficiency of GPNMB in 621-101 cells treated with non-specific (NSP) siRNA or *GPNMB* specific siRNA. **B.** Relative absorbance for the BRDU proliferation assay. Paired t-test for 4 experiments (5 replicates per experiment). ns=not significant. **C.** Relative absorbance for the MTT cell metabolic rate assay. Cells were plated for 72 hours before the addition of MTT. n=5 (5 replicates per experiment). Paired t- test. **D.** Representative images of transwell migration assay. **E.** Cell migration relative to NSP, n=3 (2 replicates per experiment with 5 images averaged per transwell). Paired t-test. **F.** Representative images of transwell invasion assay. **G.** Cell invasion relative to NSP, n=4 (2 replicates per experiment with 5 images averaged per transwell). Paired t-test.

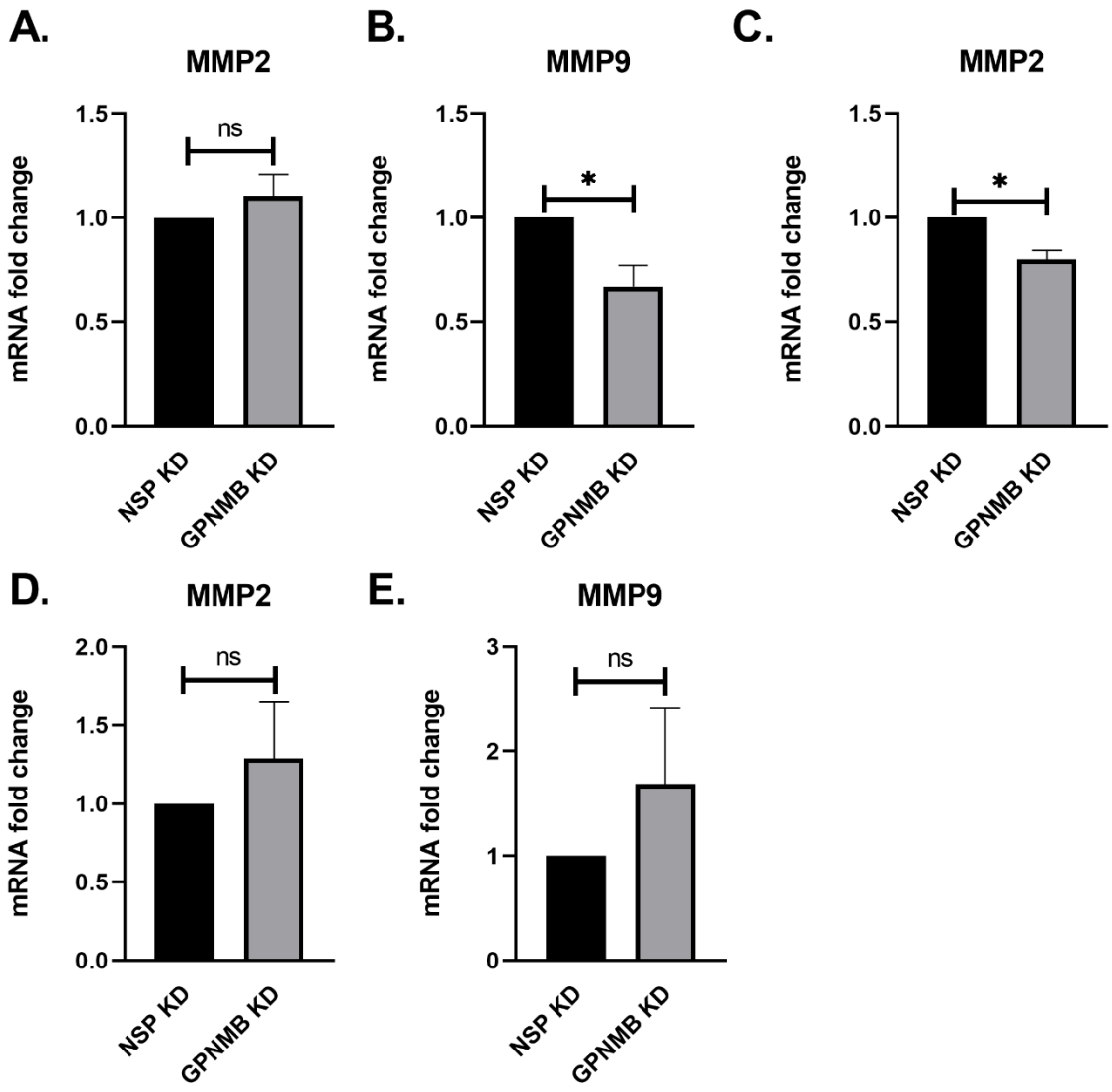

Supplemental Figure 3. **Metalloproteinase (*Mmp*) mRNAs are moderately decreased in ELT3 and LTM3 cells.** mRNA fold change of MMP2 or MMP9 determined by RT-qPCR for non-specific (NSP) and GPNMB siRNA treated cells. NSP treated samples were normalized to 1. n=3 for all experiments, except n= 4 for ELT3 MMP9. Unpaired t-test (*p<0.05). **A-B** ELT3 cells. **C.** LTM3 cells. **D-E** 621-101 cells.

Accepted Manuscript published as ERC-23-0312.R1. Accepted for publication: 11-Apr-2024

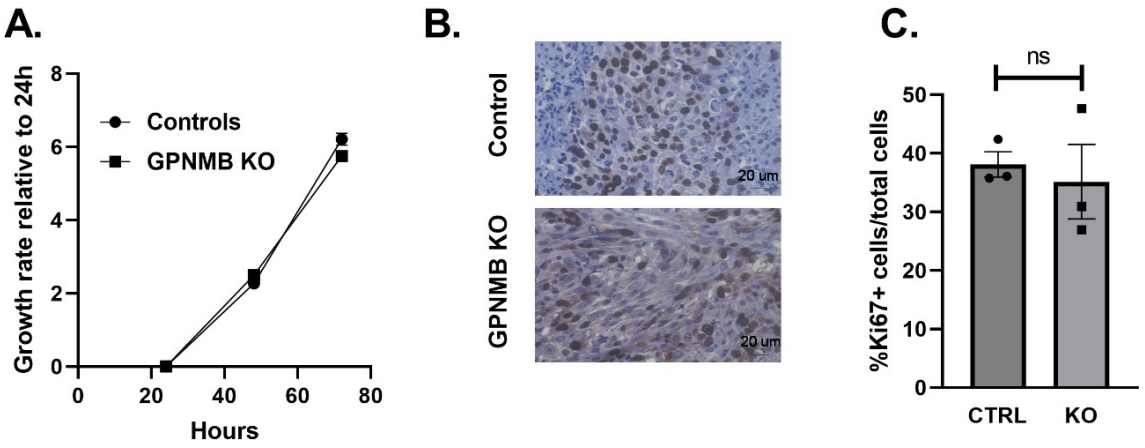

Supplemental Figure 4. **CRISPR-mediated GPNMB knockout ELT3-Luc cells proliferate at the same rate as control ELT3-luc cells *in vitro* and *in vivo*. A.** Control and GPNMB knockout (KO) cells were plated and then counted using the Celigo image cytometer at 24, 48, and 72 hours. Growth rate was compared to 24 hours for 3 control and 3 GPNMB KO cell lines. **B.** Representative 40x images of Ki67 immunohistochemistry staining for one control and one knockout tumor. **C.** Average percent of Ki67 positive cells relative to total cells three control and three knockout tumors (five images at 40x magnification counted per tumor). ns=non-significant.

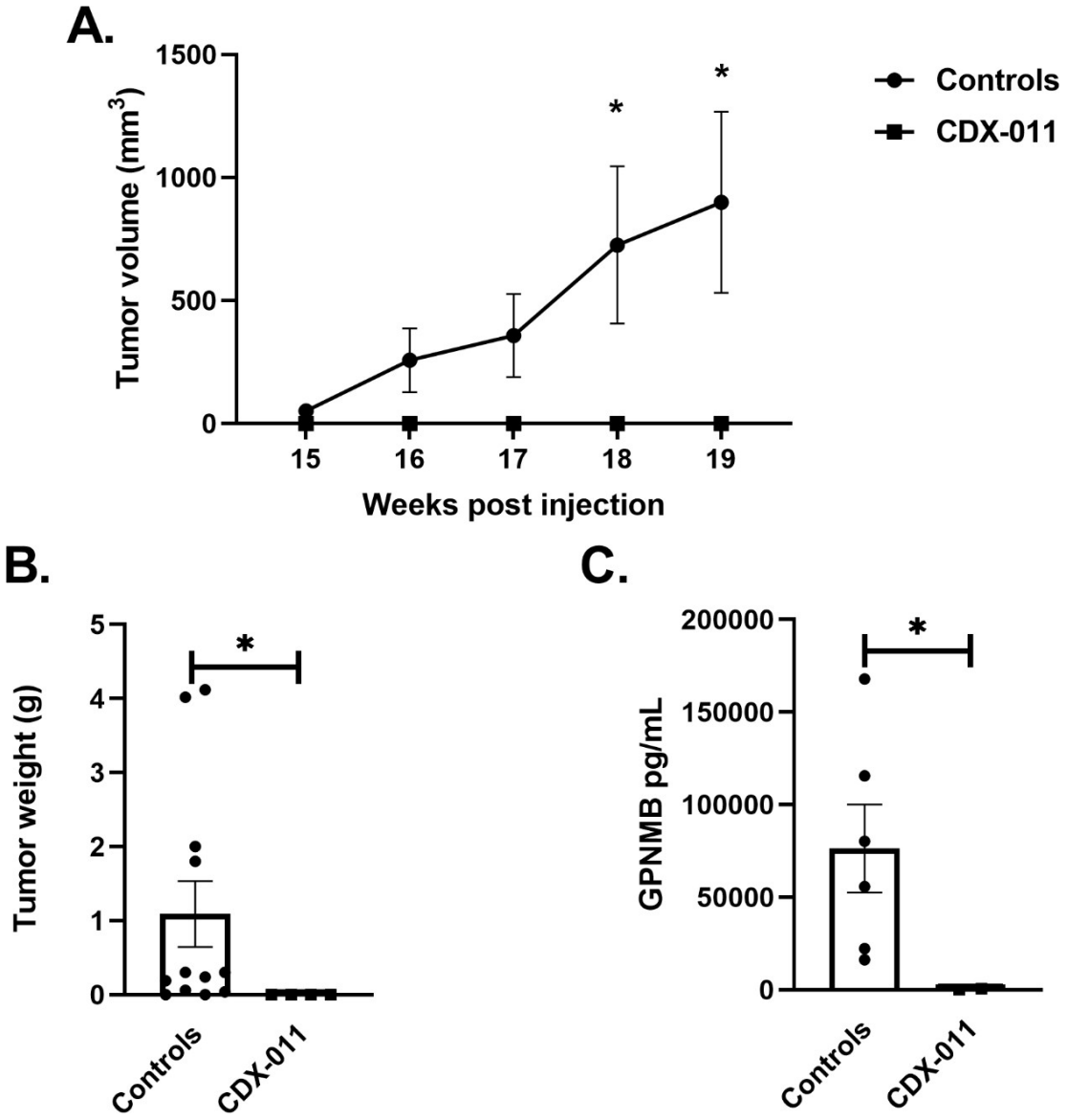

Supplemental Figure 5. **GPNMB antibody drug conjugate (CDX-011) treatment abrogates human 621-101 xenograft growth in SCID-NOD mice.** $1.94x10^6$ 621-101 cells were injected into both flanks of SCID-NOD mice. When tumors were palpable (8 weeks post injection) two mice were treated with 20 µg/100 µl CDX-011 IP (four tumors), four mice were treated with vehicle (PBS) (eight tumors) and 2 mice were given no treatment (NT, four tumors) (NT and PBS were combined for the control group analysis, 12 tumors total). Treatment occurred once a week for five weeks until 12 weeks post injection. **A.** Mean tumor volume with SEM from 12-16 weeks calculated with the formula $(L*(W)^2)/2$. Individual t-tests were run for each time point n= 12 control tumors, n=4 CDX-011 treated tumors. **B.** Final tumor weight in grams graphed with SEM, n= 12 controls, n=4 CDX-011 treated mice. **C.** Human GPNMB ELISA for serum from six control mice and two CDX-011 mice unpaired two-tailed t-test (*$p<0.05$).

Accepted Manuscript published as ERC-23-0312.R1. Accepted for publication: 11-Apr-2024

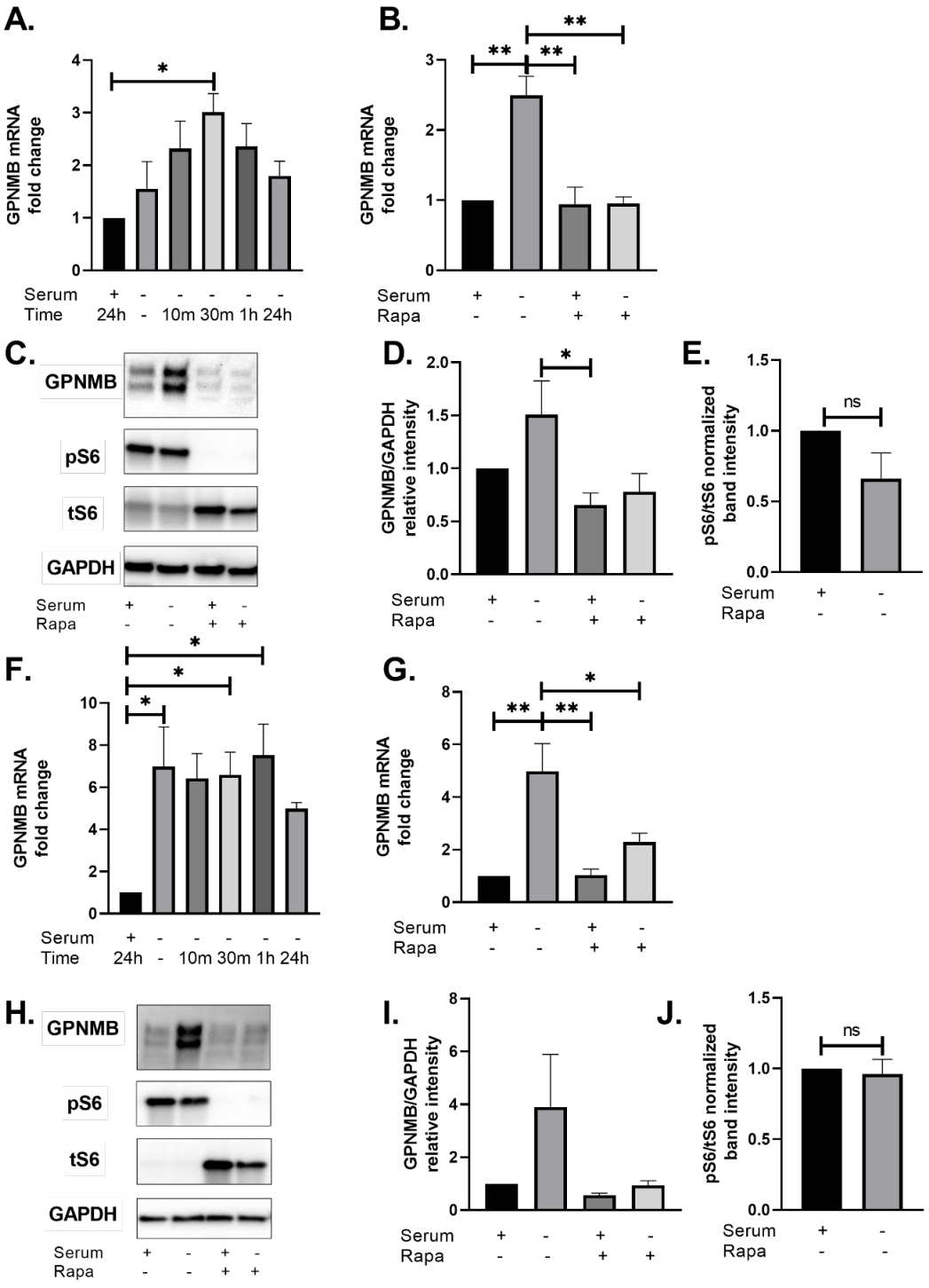

Supplemental Figure 6. **Serum Starvation increases GPNMB in mouse LTM3 and human 621-101 cells and is mTORC1- dependent. A.** mRNA Fold-change of *Gpnmb* relative to *Gapdh* mRNA determined by RT-qPCR for LTM3 cells in complete media (serum), serum starved for 24 hours, and then serum starved for 24 hours with FBS added back for 10 minutes, 30 minutes, 1 hour, or 24 hours. **B.** LTM3 cells were treated with EtOH (control) or 20uM Rapamycin (Rapa) for 24 hours in complete media or serum-free media and GPNMB mRNA fold change was calculated using RT-qPCR. **C.** Representative western Blot of the same conditions from (B). **D.** Quantification of protein samples by western blot for the same conditions as C. n=3 **E.** pS6/tS6 western blot band intensities normalized to complete media with vehicle (+serum, -Rapa). (same samples as

D) Paired t-test, ns=non-significant. **F.** RNA fold change of GPNMB relative to GAPDH determined by RT-qPCR for 621-101 cells for the same conditions as A. **G.** 621-101 cells were treated with EtOH (control) or 20uM Rapamycin (Rapa) for 24 hours in complete media or serum-free media and GPNMB mRNA fold change was calculated using RT- qPCR. **H.** Representative western Blot of the same conditions from (F). **I.** Quantification of protein samples by western blot for the same conditions as G. n=5 **J.** pS6/tS6 western blot band intensities normalized to complete media with vehicle (+serum, -Rapa). (same samples as I) Paired t-test, ns=non-significant.